Extracellular Mg^{2+} Modulates Slow Gating Transitions and the Opening of *Drosophila* Ether-à-Go-Go Potassium Channels

Chih-Yung Tang,* Francisco Bezanilla,*‡ and Diane M. Papazian*§

From the *Department of Physiology and ‡Department of Anesthesiology, and the §Molecular Biology Institute, University of California, Los Angeles School of Medicine, Los Angeles, California 90095-1751

abstract We have characterized the effects of prepulse hyperpolarization and extracellular Mg^{2+} on the ionic and gating currents of the *Drosophila* ether-à-go-go K$^+$ channel (eag). Hyperpolarizing prepulses significantly slowed channel opening elicited by a subsequent depolarization, revealing rate-limiting transitions for activation of the ionic currents. Extracellular Mg^{2+} dramatically slowed activation of eag ionic currents evoked with or without prepulse hyperpolarization and regulated the kinetics of channel opening from a nearby closed state(s). These results suggest that Mg^{2+} modulates voltage-dependent gating and pore opening in eag channels. To investigate the mechanism of this modulation, eag gating currents were recorded using the cut-open oocyte voltage clamp. Prepulse hyperpolarization and extracellular Mg^{2+} slowed the time course of ON gating currents. These kinetic changes resembled the results at the ionic current level, but were much smaller in magnitude, suggesting that prepulse hyperpolarization and Mg^{2+} modulate gating transitions that occur slowly and/or move relatively little gating charge. To determine whether quantitatively different effects on ionic and gating currents could be obtained from a sequential activation pathway, computer simulations were performed. Simulations using a sequential model for activation reproduced the key features of eag ionic and gating currents and their modulation by prepulse hyperpolarization and extracellular Mg^{2+}. We have also identified mutations in the S3–S4 loop that modify or eliminate the regulation of eag gating by prepulse hyperpolarization and Mg^{2+}, indicating an important role for this region in the voltage-dependent activation of eag.

key words: gating currents • prepulse hyperpolarization • activation model • voltage clamp

INTRODUCTION

Voltage-gated ion channels play a crucial role in determining the resting membrane potential, shaping the action potential, and controlling secretion in excitable cells. In response to depolarization of the membrane, voltage-gated channels undergo conformational changes that lead to the opening of the ion conduction pore. This sensitivity of protein conformation to changes in the transmembrane electric field is conferred by an intrinsic, charged voltage sensor (Hodgkin and Huxley, 1952; Stühmer et al., 1989; Papazian et al., 1991; Liman et al., 1991; Yang and Horn, 1995; Larsson et al., 1996; Mannuzzu et al., 1996; Yang et al., 1996; Cha and Bezanilla, 1997; Starace et al., 1997). Conformational changes of the charged voltage sensor in the electric field produce transient currents called gating currents (Schneider and Chandler, 1973; Armstrong and Beza-

nilla, 1973). Whereas measurements of ionic currents primarily yield information about the open conformation, gating current measurements provide additional information on voltage-dependent transitions between closed states that must occur before opening. These transitions constitute the essential process underlying the voltage-dependent gating of ion channels (Papazian and Bezanilla, 1997).

The voltage sensor and its conformational changes have been extensively studied in *Shaker* K$^+$ channels. K$^+$ channels comprise four similar or identical subunits that surround the water-filled pore for K$^+$ permeation (MacKinnon, 1991). In *Shaker* channels, ~13 elementary charges cross the transmembrane field during activation of a single channel (Schoppa et al., 1992). At least three positively charged residues in the S4 transmembrane segment contribute the bulk of these charges (Aggarwal and MacKinnon, 1996; Seoh et al., 1996). These residues traverse all or nearly all of the transmembrane field during voltage-dependent activation (Larsson et al., 1996; Starace et al., 1997, 1998; Starace and Bezanilla, 1998). In the tetrameric channel, these residues can therefore account for ~12 gating charges. In addition, a conserved negatively charged amino acid in the S2 transmembrane segment contributes to the gating charge of the channel (Seoh et al., 1996), but it

is currently unknown whether this residue traverses the field or instead influences the local potential experienced by the S4 residues.

The *Drosophila* ether-à-go-go K^{+} channel (eag)[1] and its vertebrate homologues constitute a unique subfamily of voltage-gated K^{+} channels (Warmke et al., 1991; Brüggemann et al., 1993; Warmke and Ganetzky, 1994). The activity of eag is controlled by changes in the membrane potential, and it contains the charged residues in S2 and S4 that constitute the voltage sensor in other K^{+} channels. A unique feature of eag and its homologues is that extracellular Mg^{2+} regulates the kinetics of channel activation (Terlau et al., 1996; Meyer and Heinemann, 1998; Frings et al., 1998), leading to the proposal that Mg^{2+} modulates the intrinsic, voltage-dependent gating mechanism of eag family members (Terlau et al., 1996). To test this hypothesis, we have compared the effects of Mg^{2+} and prepulse hyperpolarization on the ionic and gating currents of eag. Our results confirm that Mg^{2+} regulates transitions in the activation pathway of eag. In addition, Mg^{2+} controls the kinetics of pore opening.

MATERIALS AND METHODS

Molecular Biology

Wild-type eag channels and the mutants L342H and Δ333-337 were expressed in *Xenopus* oocytes as previously described (Tang and Papazian, 1997). The appropriate cDNA subclones were linearized with NotI for in vitro transcription using the mMESSAGE mMACHINE kit (Ambion Inc.). RNA was injected into oocytes for electrophysiological analysis of channel activity 1–4 d later.

Electrophysiology

Ionic and gating currents from wild-type and L342H channels were measured using the cut-open oocyte vaseline gap technique (Stefani et al., 1994). Ionic currents from Δ333–337 channels were recorded using a conventional two-electrode voltage clamp (Timpe et al., 1988). All experiments were performed at room temperature (19–21°C).

In experiments using a two-electrode voltage clamp, pipettes were filled with 3 M KCl. The bath contained normal Ringer's solution, composed of 118 mM NaCl, 1.8 mM $CaCl_2$, and 10 mM HEPES, pH 7.2. As noted, NaCl was replaced by KCl to record eag tail currents, and $MgCl_2$ was added to investigate the effect of Mg^{2+} on activation of eag channels. Voltage-clamp protocols were applied and data were acquired using pCLAMP v.5.5.1 software and a TL-1 Labmaster Interface (Axon Instruments). Linear leak and capacitive currents were subtracted using the P/−4 protocol (Bezanilla and Armstrong, 1977). The holding potential for subtraction was −100 or −110 mV.

In experiments using the cut-open oocyte voltage clamp, pipettes were filled with 3 M KCl or 3 M NaCl. Electrical access to the interior of the oocyte was achieved by permeabilizing the membrane with 0.1% saponin applied in the lower chamber. To record ionic currents, the extracellular solution contained 120 mM Na-methanesulfonate (MES) or 120 mM *N*-methylglucamine (NMG)-MES, 1.8 mM $CaCl_2$, and 10 mM HEPES, pH 7.2. The in-

ternal solution contained 120 mM K-MES, 1 mM EGTA, and 10 mM HEPES, pH 7.2. Extracellular Na-MES or NMG-MES was replaced by K-MES to record tail currents, and 2 mM $MgCl_2$ was added to the extracellular solution as noted. To measure gating currents, ionic currents were blocked by replacing the external Na-MES or NMG-MES and internal K-MES with TEA-MES. Linear leak and capacitive currents were subtracted using the P/−4 protocol with a subtraction holding potential of −110 mV (Bezanilla and Armstrong, 1977). Data were filtered at 2–5 kHz and digitized at a frequency five times higher than the filter frequency using an interface made in the Bezanilla laboratory. Data acquisition and analysis programs were written in the Bezanilla laboratory.

To study the effect of hyperpolarizing prepulses on gating current kinetics, leak and capacitive currents were compensated electronically at 0 mV. In control experiments, we attempted to detect gating charge movement between −200 and −100 mV using a variety of alternative subtraction protocols, including (a) P/−4 with subtracting holding potentials as negative as −180 mV, (b) P/+4 with subtracting holding potentials up to +10 mV, and (c) no subtraction (electronic compensation at 0 mV). Substantially similar results were obtained regardless of the subtraction protocol (data not shown).

The kinetics of eag ionic and gating currents were described by fitting specified regions of the current traces with a single exponential function using our own analysis software or Origin software (Microcal Software, Inc.). For gating currents, the decaying phases of both ON and OFF gating currents were fitted. For ionic currents, the late rising phase (close to the peak) of activation currents and the decaying phase of tail currents were fitted.

ON and OFF gating charge was measured by time integration of the ON and OFF gating currents using our own analysis software.

Computer Simulations

The SCOP v. 3.5 simulation program (Simulation Resources) was used to simulate eag ionic and gating currents using a modified kinetic scheme based on the class D model for the *Shaker* channel proposed by Zagotta et al. (1994b). For a given transition, i, the voltage-dependent forward (α_i) and backward (β_i) rate constants were assumed to take the form: $\alpha_i = \alpha_{i0}\exp(z_{fi}eV/kT)$, and $\beta_i = \beta_{i0}\exp(-z_{bi}eV/kT)$, where α_{i0} and β_{i0} are the rates at 0 mV, z_{fi} and z_{bi} are the valences of the moving charge in the forward and backward directions, e is the elementary charge (1.6×10^{-19} C), V is the membrane potential, and k and T are the Boltzmann constant and absolute temperature, respectively.

RESULTS

Effect of Prepulse Hyperpolarization on eag Ionic Current Kinetics

As originally shown by Cole and Moore (1960), hyperpolarizing prepulses modulate the kinetics of K^{+} channel opening in response to a subsequent depolarization. In a variety of voltage-dependent K^{+} channels, including the squid axon delayed rectifier and the *Shaker* channel, hyperpolarizing prepulses delay the onset, but do not significantly change the time course of ionic current activation (Cole and Moore, 1960; Stefani et al., 1994; Zagotta et al., 1994a; Schoppa and Sigworth, 1998). This phenomenon provides evidence that channel proteins transit through several closed conformations before opening (Cole and Moore, 1960; Stefani et al., 1994; Zagotta et al., 1994a; Schoppa and Sigworth, 1998).

---

[1]*Abbreviations used in this paper:* eag, *Drosophila* ether-à-go-go K^{+} channel; MES, methanesulfonate.

The *Drosophila* eag K$^+$ channel was expressed in *Xenopus* oocytes to investigate the effects of prepulse hyperpolarization on the ionic current. Hyperpolarizing prepulses delayed the onset of channel opening and, in addition, dramatically slowed the kinetics of the ionic currents evoked by a subsequent depolarization (Fig. 1 A). As a result, eag ionic currents elicited after various prepulses could not be superimposed by shifting the traces along the time axis (Fig. 1 B). This phenomenon

has been attributed to the existence of rate-limiting transitions between remote closed states reached only during hyperpolarizations (Young and Moore, 1981). Therefore, these results suggest that the eag channel moves through a series of closed states before opening, and that transitions between closed states populated at hyperpolarized potentials are rate limiting for the activation process. Hyperpolarizing prepulses similarly modulate the kinetics of mammalian eag homologues
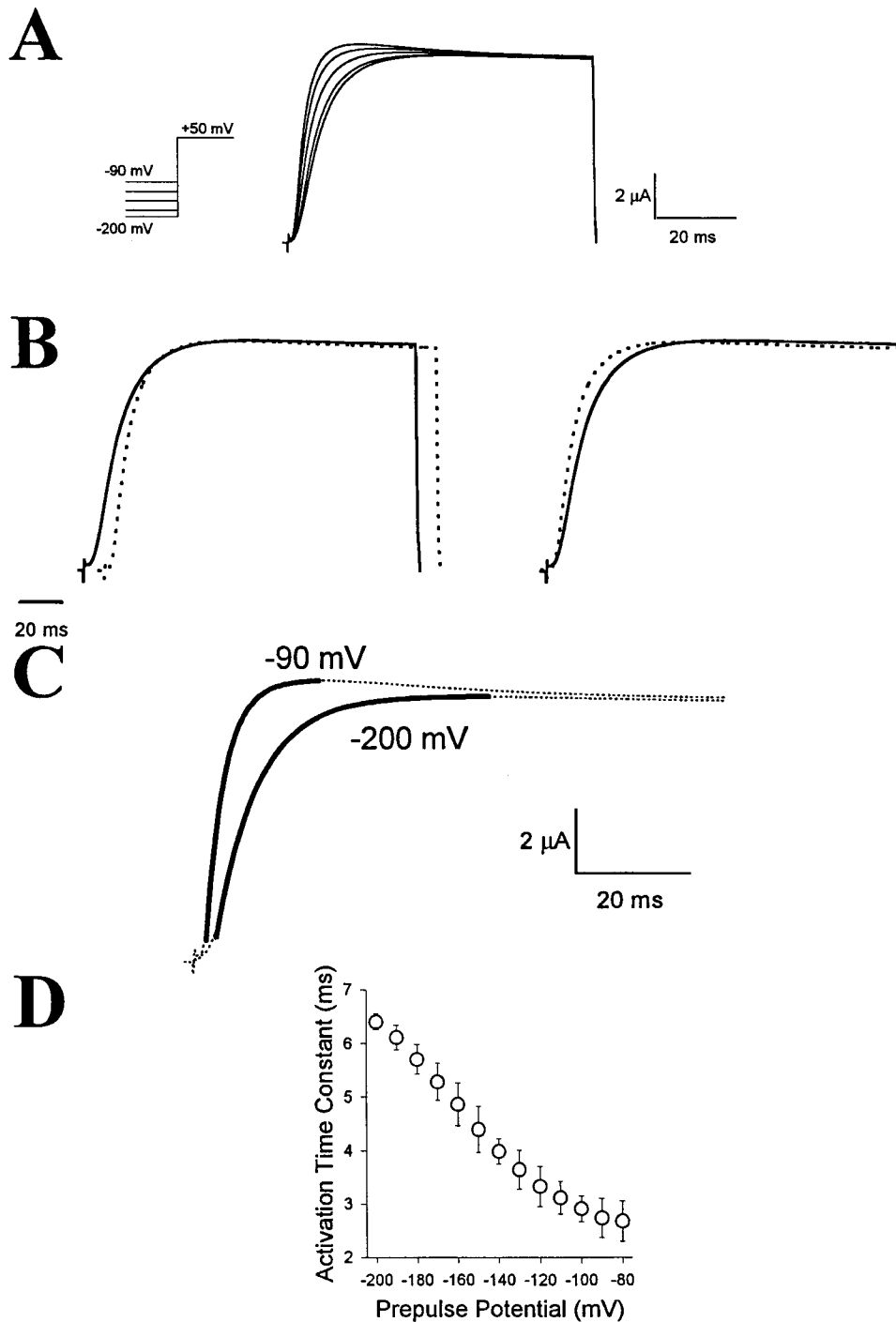

Figure 1. Prepulse hyperpolarization slows activation of eag ionic currents. (A) From a holding potential of −90 mV, 75-ms hyperpolarizing prepulses ranging from −200 to −90 mV were applied in 20- or 30-mV increments, followed by a test pulse to +50 mV. Representative currents evoked by the test pulses are shown. After more negative prepulses, the time course of the ionic current was slower. (B) The time course of the rising phase of the ionic current after prepulses to −200 mV (solid line) and −150 mV (dashed line) cannot be superimposed by shifting the traces along the time axis. The traces were scaled and aligned at either the peak (left) or foot (right) of the rising phase. (C) Fits with a single exponential function (solid lines) to the late phase of activation are shown superimposed on ionic current traces (dashed lines) after prepulses to −90 or −200 mV. (D) Activation time constants at +50 mV obtained from single exponential fits to the late rising phase of the eag ionic current are plotted versus prepulse potential. Data are shown as mean ± SEM, *n* = 6.

(Ludwig et al., 1994; Robertson et al., 1996; Terlau et al., 1996; Frings et al., 1998; Meyer and Heinemann, 1998).

The initial phase of activation in the eag channel and its mammalian homologues displays sigmoid kinetics (Ludwig et al., 1994; Terlau et al., 1996). As a result, multiple exponential components are needed to provide an adequate fit of eag ionic currents. However, the late phase of activation is well fitted by a single exponential function. Therefore, that phase was fitted to quantify activation kinetics as a function of prepulse potential (Fig. 1 C). As the prepulse potential was varied from -80 to -200 mV, the activation time constant in response to a test pulse to $+50$ mV more than doubled, increasing from <3 to >6 ms (Fig. 1 D).

Effect of Extracellular Mg^{2+} on eag Ionic Currents

Without applying hyperpolarizing prepulses, eag ionic currents were dramatically slowed in the presence of 2 mM extracellular Mg^{2+} (Fig. 2 A). Steady state current amplitudes were unchanged. The effect of Mg^{2+} on channel kinetics was quantified by fitting a single exponential component to the late phase of ionic current activation (Fig. 2 B). Mg^{2+} slowed eag activation kinetics in a voltage-dependent manner, with a larger effect after smaller depolarizing steps (Fig. 2 C). At -10 mV, 2 mM Mg^{2+} increased the time constant of activation $\sim$11-fold, from $\sim$13 to 148 ms. Higher concentrations of extracellular Mg^{2+} resulted in even slower activation kinetics (data not shown).
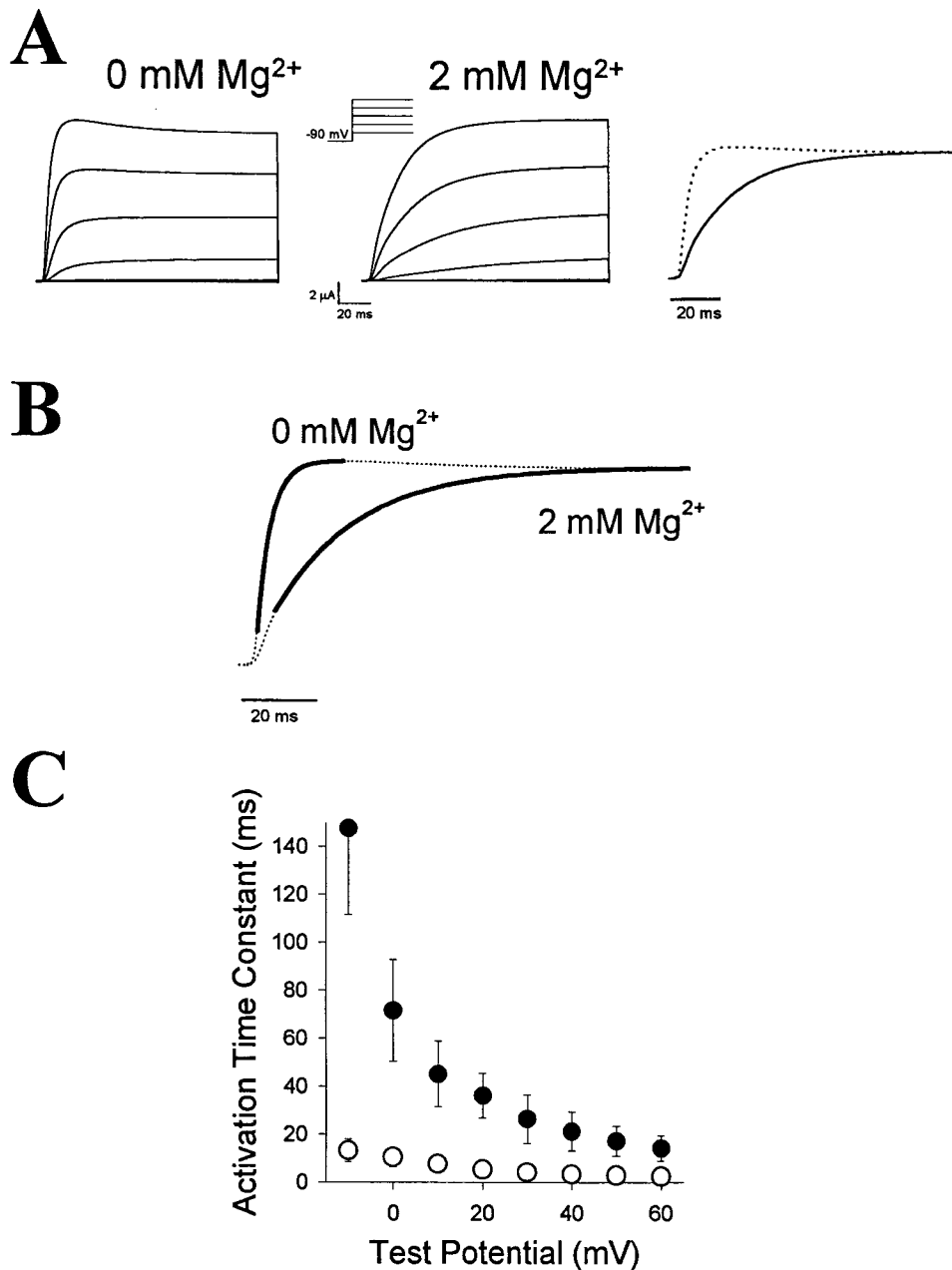

Figure 2. Extracellular Mg^{2+} slows activation of eag ionic currents. (A) From a holding potential of -90 mV, 120-ms test pulses from -60 to $+60$ mV were applied in 20-mV increments in the absence (left) or presence (middle) of 2 mM Mg^{2+} in the extracellular solution. Note that partial inactivation was sometimes observed in the absence of Mg^{2+}. (Right) Ionic current traces evoked at $+40$ mV in the absence (dashed line) and presence (solid line) of 2 mM Mg^{2+} were scaled and overlaid to compare the time course of ionic current activation. (B) Fits with a single exponential function (solid lines) are shown superimposed on the late phase of ionic current activation at $+40$ mV (dashed lines) in the absence and presence of Mg^{2+}. (C) Activation time constants at $+40$ mV obtained from single exponential fits to the late rising phase of the eag ionic current in the presence (●) and absence (○) of 2 mM Mg^{2+} are plotted versus test potential. Data are shown as mean $\pm$ SEM, $n = 7$. In this and subsequent figures, if error bars are not visible, the SEM was smaller than the size of the symbol.

In addition to decelerating activation initiated from a holding potential of -90 mV, Mg^{2+} dramatically slowed activation kinetics after hyperpolarizing prepulses (Fig. 3 A). The interaction of Mg^{2+} and prepulse hyperpolarization was complex and particularly prominent during the initial phase of activation (compare Fig. 3 B with 1 C). Because the initial phase of activation was poorly fitted by a single exponential component, the effect was quantified by measuring the time required to reach half peak current amplitude at $+50$ mV as a function of

prepulse potential in the presence and absence of Mg^{2+} (Fig. 3 C). The time to half peak is sensitive to changes in both the delay and time course of the ionic currents. The range of prepulse potentials that elicited the steepest change in the time to half peak appeared to be shifted to more depolarized values in the presence of Mg^{2+} (Fig. 3 C). The interaction of Mg^{2+} and prepulse hyperpolarization suggests that Mg^{2+} further slows rate-limiting gating transitions between closed states that are populated at hyperpolarized potentials,
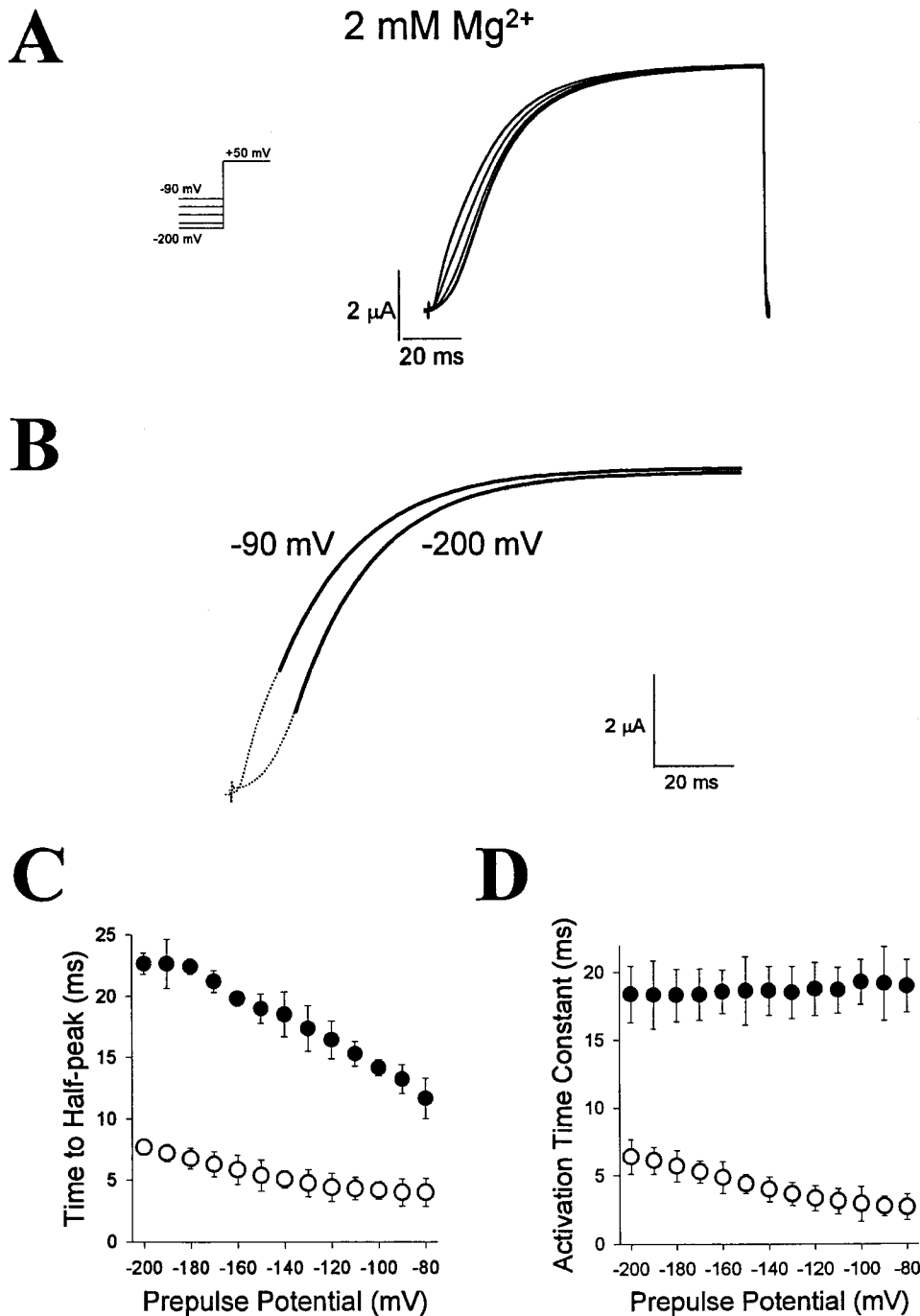

Figure 3. Extracellular Mg^{2+} enhances the effect of prepulse hyperpolarization on eag ionic currents. (A) Current traces evoked in the presence of 2 mM Mg^{2+} by a test pulse to $+50$ mV after hyperpolarizing prepulses to potentials from -90 to -200 mV are shown. The pulse protocol was the same as in Fig. 1 A. (B) Fits with a single exponential function (solid lines) to the late phase of activation are shown superimposed on ionic current traces (dashed lines) after prepulses to -90 or -200 mV. (C) The time to half maximal current amplitude at $+50$ mV was measured in the presence ($\bullet$) and absence ($\bigcirc$) of 2 mM Mg^{2+} and plotted versus prepulse potential. Data are shown as mean $\pm$ SEM, $n = 5$. (D) Activation time constants at $+50$ mV obtained from single exponential fits to the late rising phase of the eag ionic current in the presence ($\bullet$) and absence ($\bigcirc$) of 2 mM Mg^{2+} are plotted versus prepulse potential. Data are shown as mean $\pm$ SEM, $n = 5$.

and may shift the voltage dependence of these transitions in the depolarized direction.

The late phase of ionic current activation was fitted with a single exponential component (Fig. 3 B), and the resulting time constants were plotted versus prepulse potential (Fig. 3 D). During the late phase of activation, the dramatic slowing of activation kinetics by Mg^{2+} was virtually independent of prepulse potential.

A reactivation protocol was used to investigate the effect of Mg^{2+} on other transitions in the activation pathway (Oxford, 1981). Two identical pulses to +50 mV were applied, separated by a variable interpulse interval at −90 mV, a potential at which the channel deactivates (Fig. 4 A). This protocol provides several kinds of information. First, it can determine whether the opening transition is rate limiting for activation. During very short interpulse intervals, most channels will return only to the nearest closed state or states, so that as the interpulse interval becomes shorter, the activation kinetics will approach those of the opening transition measured in isolation. If the opening is rate limiting, the time course of activation will be identical during the first and second pulses, regardless of the interpulse interval. Second, it can determine whether Mg^{2+} alters the rate of the opening transition, estimated during the second pulse at very short interpulse intervals. Finally, the interpulse interval needed to return to the original activation kinetics provides information about the time course of back transitions between closed states en route to the rate-limiting transition for activation.

To determine whether the opening transition was rate limiting, the time courses of activation during the first and second depolarizing pulses were compared. At very short interpulse intervals, eag opened more quickly in response to the second pulse compared with the first in both the presence and absence of Mg^{2+} (Fig. 4 A). Therefore, the opening transition is not the rate limiting step for eag activation.

The cut-open oocyte voltage clamp provides excellent temporal resolution, making it feasible to measure reactivation time constants after interpulse intervals as short as 0.1 ms. During extremely short interpulse intervals, many channels do not close. The experiment was therefore performed using a bath solution nominally free of K^+ to eliminate inward currents at −90 mV, which would interfere with determining reactivation kinetics after short interpulse intervals.

In the absence of external Mg^{2+}, the fitted reactivation time constant was ∼0.5 ms after an interval of 0.1 ms, and reached 3 ms after an interval of 1 ms. In contrast, in the presence of 2 mM Mg^{2+}, the reactivation time constant was ∼5 ms within the same range of interpulse intervals (Fig. 4 B), and remained at this value for intervals as long as 30 ms (data not shown). These results suggest that Mg^{2+} modulates the kinetics of

channel opening in eag. In contrast, Mg^{2+} did not change the kinetics of deactivation, indicating that Mg^{2+} does not modulate the transition from the open state to the most accessible closed state(s) (Fig. 4 C).

In the absence of external Mg^{2+}, activation kinetics during the second pulse matched those of the first pulse after interpulse intervals longer than 2 ms. In contrast, in the presence of 2 mM Mg^{2+}, interpulse intervals of >600 ms were required for the activation kinetics to return to their original rate (Fig. 4 D). These results indicate that one or more back transitions between closed states are slowed by extracellular Mg^{2+}.

The results presented so far indicate that Mg^{2+} modulates activation gating in eag K^+ channels, as previously suggested for the rat homologue of eag (Terlau et al., 1996). In particular, our data suggest that Mg^{2+} modulates at least two steps in the activation pathway, rate-limiting transitions between closed states populated at hyperpolarized potentials, as well as the transition from a nearby closed state(s) to the open state. To investigate how Mg^{2+} affects the intrinsic voltage-dependent gating process, eag gating currents were characterized.

Measurement of eag Gating Currents

eag ionic currents were blocked by perfusing the oocyte both externally and internally with TEA, and gating currents were recorded with the cut-open oocyte voltage clamp (Fig. 5 A). In response to depolarizing pulses, a small rising phase was observed in the ON gating currents, indicating that initial transitions in the activation pathway move less charge than subsequent transitions. Rising phases have also been observed in gating currents recorded from *Shaker* and Kv2.1 K^+ channels (Bezanilla et al., 1991; Taglialatela and Stefani, 1993; Stefani et al., 1994). Upon repolarization, OFF gating currents were recorded. The time course of OFF gating currents was slower for larger depolarizations, which lead to channel opening, suggesting that the return of the gating charge is delayed once the channel reaches the open state (Fig. 5 B). A similar phenomenon has been observed in other voltage-dependent K^+ channels (Taglialatela and Stefani, 1993; Stefani et al., 1994; Zagotta et al., 1994a; Chen et al., 1997; Schoppa and Sigworth, 1998).

The steady state activation properties of eag channels were characterized by deriving open probability–voltage (P_o-V) and gating charge–voltage (Q-V) curves from ionic and gating currents, respectively (Fig. 5 C, and Table I). In Fig. 5, the Q-V curve plots the OFF gating charge (Q_{OFF}), obtained as the time integral of the OFF gating current, as a function of pulse potential. Each curve was fitted with a single Boltzmann distribution to derive a midpoint potential (V_{mid}) and apparent gating valence (z). Consistent with the existence of several closed states in the activation
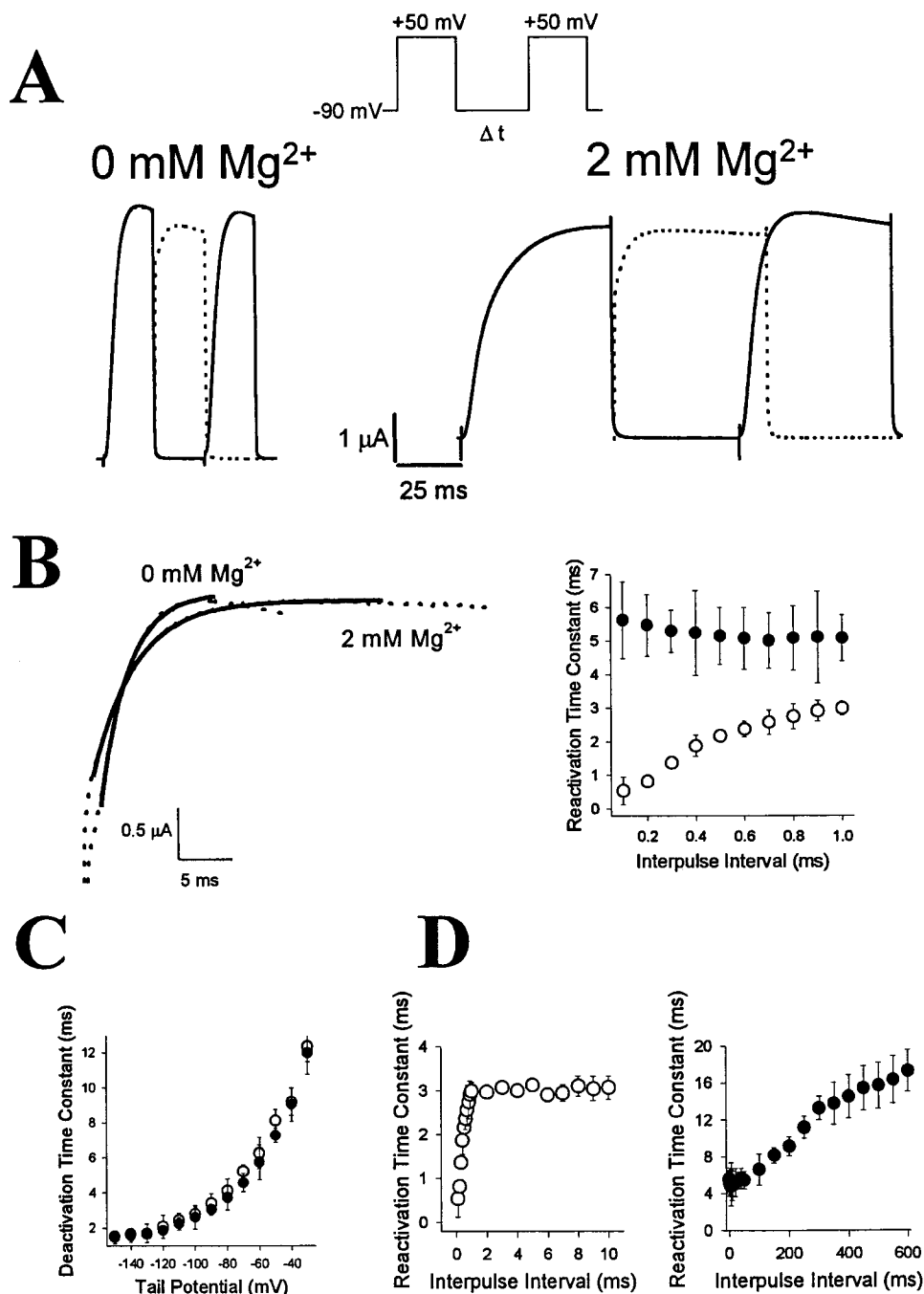
Figure 4. Extracellular Mg^{2+} slows opening of the channel and back transitions between closed states. (A, top) The voltage protocol for the reactivation experiment is shown. From a holding potential of -90 mV, two identical test pulses to $+50$ mV separated by a variable interpulse interval (Δt) at -90 mV were applied. Test pulse duration was 20 or 70 ms in the absence or presence of 2 mM Mg^{2+}, respectively. The experiment was performed using a nominally K^+-free bath solution to eliminate inward tail currents at -90 mV, which would interfere with detecting reactivation after short interpulse intervals. (Bottom) Representative current traces evoked by the reactivation protocol in the absence of Mg^{2+} (left) were obtained using $\Delta t = 0.5$ ms (dashed traces) or 20 ms (solid traces). Representative current traces evoked by the reactivation protocol in the presence of 2 mM Mg^{2+} (right) were obtained using $\Delta t = 1$ ms (dashed traces) or 50 ms (solid traces). (B, left) The late rising phase of currents evoked by the second test pulse (dashed traces) in the presence and absence of Mg^{2+}, as indicated, were fitted with single exponential functions (solid lines). In the representative experiment shown, $\Delta t = 1$ ms. (Right) Fitted time constants for the second test pulse were determined for short interpulse intervals (between 0.1 and 1 ms) in the presence (●) and absence (○) of 2 mM Mg^{2+} and plotted versus Δt. Data are shown as mean $\pm$ SEM, $n = 3$. (C) Tail currents were recorded in the presence (●) or absence (○) of 2 mM Mg^{2+} by stepping from $+50$ mV to potentials ranging from -90 to -150 mV. Deactivation time constants were derived from single exponential fits and plotted versus tail potential. (D) Mg^{2+} slows the time course of the return to the original activation kinetics. Fitted time constants for the second test pulse were determined as shown in B in the presence (●) and absence (○) of 2 mM Mg^{2+} and plotted versus Δt. Note that the graphs have different scales for both the ordinate and the abscissa. Data are shown as mean $\pm$ SEM, $n = 3$.

pathway, V_{mid} for the Q-V curve was shifted by -20 mV relative to V_{mid} for the P_o-V curve. The Q-V curve was slightly steeper, as reflected in its higher z value. Lower estimates of the gating valence for the Q-V and P_o-V curves corresponded to ~2.5 and 2.1 e_0, respectively. Extracellular Mg^{2+} (2 mM) shifted the P_o-V and Q-V curves by <5 or 10 mV in the depolarized direction (Fig. 5 D).

Q-V curves derived from ON and OFF gating currents are expected to be identical. In some types of channels, however, Q_{ON} and Q_{OFF} cannot be measured with equal accuracy. In the eag channel, the kinetics of the ON gating current were slow, particularly for depolarizations to 0 mV or less, leading to underestimates of the ON gating charge. The slow movement of the ON charge
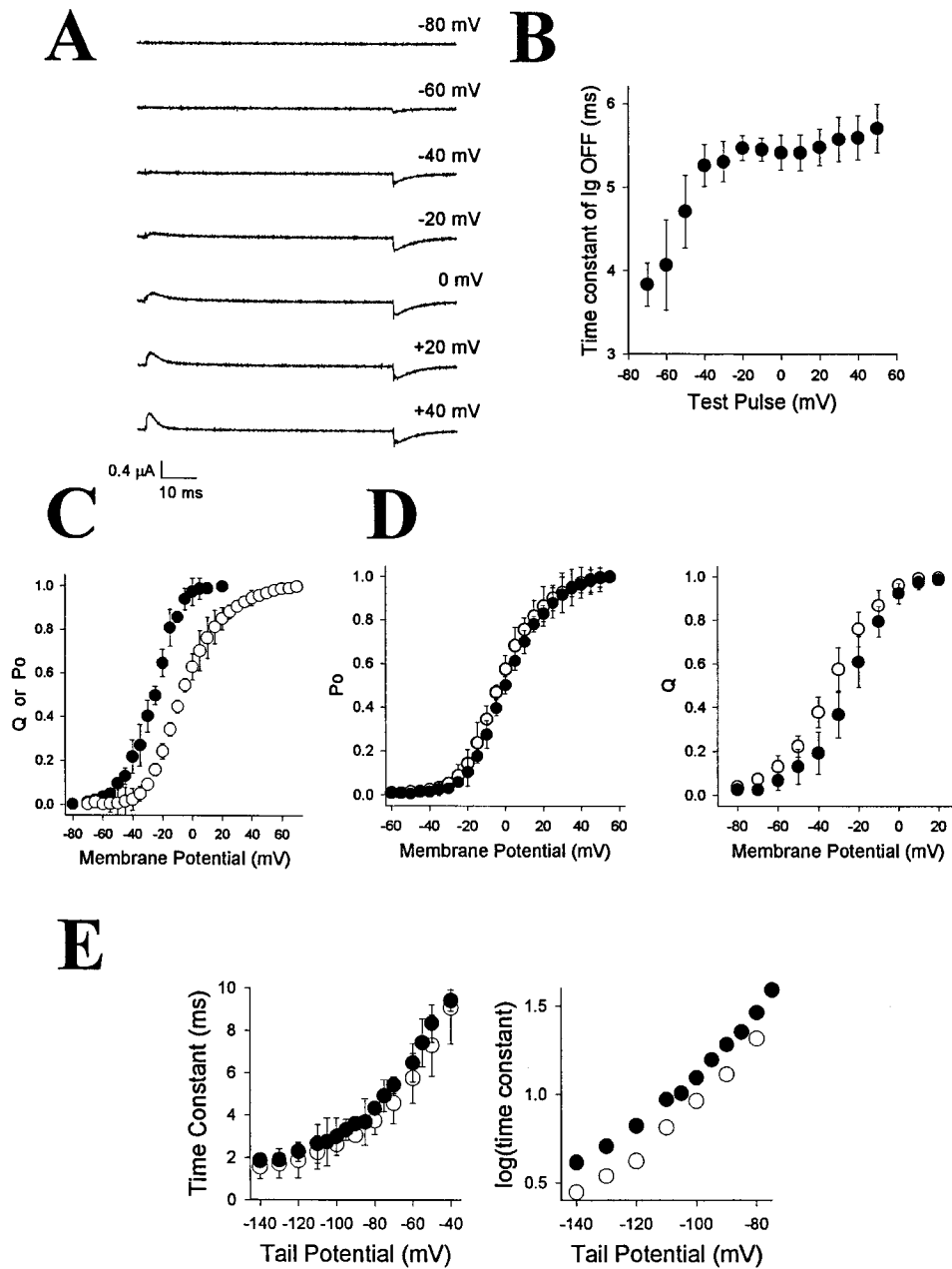
Figure 5. Characterization of eag gating currents. (A) From a holding potential of -90 mV, 70-ms test pulses to the indicated potentials were applied using the cut-open oocyte voltage clamp. Representative gating current traces are shown. (B) After test pulses to various potentials, OFF gating currents were recorded upon return to -90 mV. A single exponential component was fitted to the decaying phase of the OFF gating current to obtain a time constant, which was plotted versus test potential. Data are shown as mean $\pm$ SEM, $n = 5$. (C) Steady state activation curves of eag gating (Q-V, ●) and ionic (P_o-V, ○) currents. For the Q-V curve, OFF gating currents elicited by 70-ms pulses to the indicated test potentials were integrated to obtain Q_{OFF}, which was normalized to the maximal value obtained in each experiment. The P_o-V curve was obtained from normalized isochronal tail currents. Data are shown as mean $\pm$ SEM, $n = 6$ and 8 for the Q-V and P_o-V curves, respectively. (D) P_o-V (left) and Q-V (right) curves obtained in the presence (●) or absence (○) of 2 mM Mg^{2+} are shown. Data are shown as mean $\pm$ SEM, $n = 4$–6. (E) Ionic or gating currents were elicited by 70-ms pulses to $+50$ mV, followed by repolarization to a variety of tail potentials. (Left) Time constants from single exponential fits of ionic current tails (○) and OFF gating currents (●) are plotted versus tail potential. Data are shown as mean $\pm$ SEM, $n = 4$ and 3 for ionic tail currents and OFF gating currents, respectively. (Right) A semilogarithmic plot of the same data is shown. The closing valence (Zc), determined from the slope of a linear regression fit of the data, was ~0.37 for both ionic tail currents and OFF gating currents.

could be inferred from a gradual increase in the OFF gating charge with longer pulse durations, reflecting the return of additional charge (see Fig. 7 B). Therefore, to characterize the gating charge–voltage relationship of the eag channel, we measured the OFF gating charge evoked by repolarization after 70-ms pulses (Fig. 5 C). This procedure should provide an accurate estimate of the total charge because at this time point, the OFF charge movement has saturated. In eag, unlike other channels such as *Shaker*, fast inactivation and TEA do not delay the return of the OFF gating charge, a

phenomenon that has been called charge immobilization (Armstrong and Bezanilla, 1977; Bezanilla et al., 1991; Olcese et al., 1997). In eag, the ON and OFF gating charge were virtually identical at large depolarizations where the ON gating charge could be reliably estimated (data not shown). The OFF gating charge increased with pulse durations up to 70 ms, reflecting additional ON gating charge movement, and then remained constant during longer pulses (see Fig. 7 B).

In eag, ionic tail currents and OFF gating currents had similar time courses over a wide range of potentials

	V_{mid}	z
Q-V	-25.1 ± 0.3	2.5 ± 0.3
P_o-V	-4.3 ± 0.8	2.1 ± 0.2

Values for the midpoint potential (V_{mid}) and apparent gating valence (z) were derived from Q-V and P_o-V curves fit with a Boltzmann equation of the form: Q(V) or P_o(V) = $1/\{1 + \exp[(V_{mid} - V)\,ez/kT]\}$, where Q is the normalized OFF gating charge; P_o is the fraction of open channels obtained from the normalized amplitude of isochronal tail currents after a depolarization to the test potential, V; e is the elementary charge (1.6×10^{-19} C); and k and T are the Boltzmann constant and absolute temperature; respectively. Data are shown as mean $\pm$ SEM, $n = 6$ and 8 for the Q-V and P_o-V curves, respectively.

(Fig. 5 E). The closing valence (z_c) as determined from the slope of a semilogarithmic plot of time constant versus tail potential (Fig. 5 E, right) was ~0.37 in both cases. Importantly, these similarities suggest that ionic current tails and OFF gating currents are measuring the same molecular event.

Prepulse Hyperpolarization and Extracellular Mg^{2+} Modulate eag Gating Current Kinetics

Hyperpolarizing prepulses slowed the time course of the ON gating currents. Decay kinetics of ON gating currents obtained after prepulses to different potentials could not be superimposed (Fig. 6 A). At potentials more negative than -130 mV, the effect of prepulse hyperpolarization on the ON gating currents was enhanced by extracellular Mg^{2+} (Fig. 6 B). These results indicate that Mg^{2+} directly modulates the activation gating process in eag channels. In contrast, OFF gating current kinetics were unaffected by Mg^{2+} (Fig. 6 A).

Hyperpolarizing prepulses in the presence and absence of Mg^{2+} have qualitatively similar effects on the kinetics of eag ionic currents and ON gating currents (Figs. 1, 3, and 6). Quantitatively, however, the change in gating current kinetics was significantly less than that seen in the ionic currents (compare Figs. 1 D, 3 B, and 6 B). This suggests that prepulse hyperpolarization accesses gating transitions that occur slowly and/or move relatively little charge, and are therefore difficult to de-
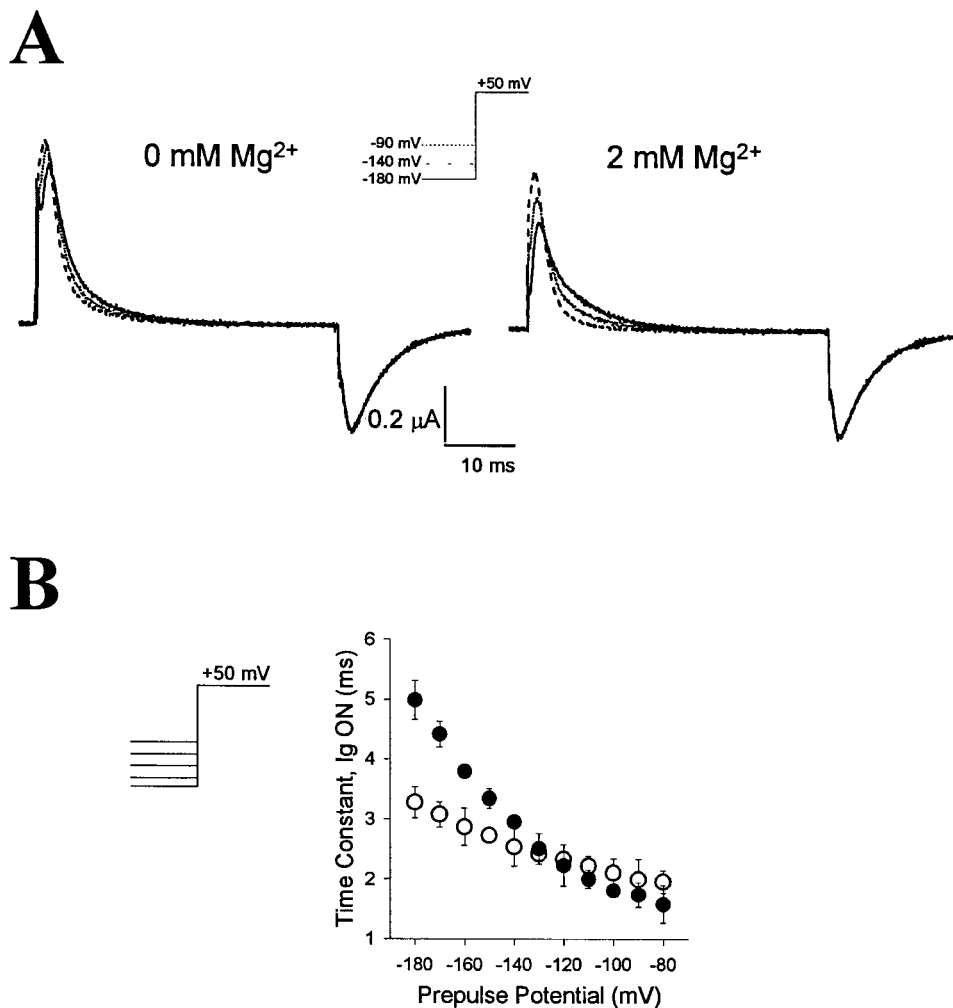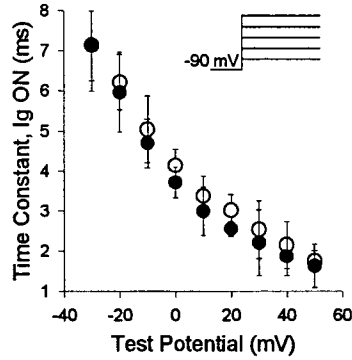

Figure 6. Extracellular Mg^{2+} enhances the effect of prepulse hyperpolarization on eag gating currents. (A) The effect of hyperpolarizing prepulses on the gating current of eag in the absence (left) or presence (right) of 2 mM Mg^{2+}. Gating currents were evoked using the same voltage protocol as in Fig. 1, except that leak and capacitative currents were compensated electronically at 0 mV. Representative traces are shown. After more negative prepulses, the time course of the decay phase of the ON gating current was slower. (B) After 75-ms prepulses to potentials between -80 and -180 mV, ON gating currents were evoked by a test pulse to $+50$ mV. The decay phase of the ON gating currents obtained in the presence ($\bigcirc$) or absence ($\bullet$) of 2 mM Mg^{2+} was fitted with a single exponential function and plotted versus prepulse potential. Data are shown as mean $\pm$ SEM, $n = 3$.
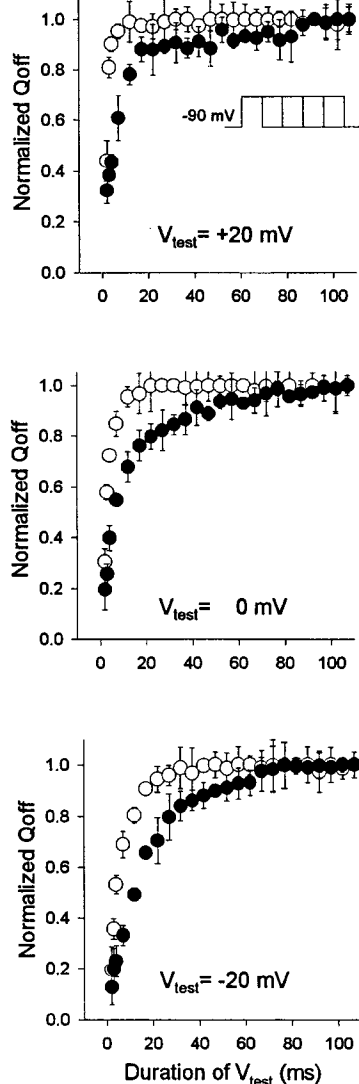
A

B

tect with gating current measurements. Attempts to detect gating charge movement between -200 and -100 mV were unsuccessful.

In the Absence of Hyperpolarizing Prepulses, the Activation Kinetics of eag Gating and Ionic Currents Show Differential Sensitivity to Extracellular Mg^{2+}

In the absence of hyperpolarizing prepulses, Mg^{2+} had significantly different effects on the ionic and gating currents of eag channels. Although extracellular Mg^{2+} dramatically slowed the activation of eag ionic currents (Fig. 2), the kinetics of the decay phase of the ON gating currents evoked by depolarizing from a holding potential of -90 mV were insensitive to Mg^{2+} (Fig. 7 A). This suggests that channel opening requires transitions that are not well represented in the gating current measurements.

ON gating currents are slow in eag channels, and therefore the effects of Mg^{2+} may be difficult to resolve. To investigate whether a slow, Mg^{2+}-sensitive component of gating charge movement is present, the magnitude of the OFF gating charge (Q_{OFF}) was measured as a function of pulse duration. Longer depolarizing pulses provide an opportunity for slow components of the ON gating charge to move. Although this charge may be lost in the baseline during integration of ON gating currents, a slow component of charge movement should be detectable as a gradual increase in Q_{OFF} as a function of pulse duration. Indeed, this protocol revealed a slow component of charge movement that was more prominent in the presence of Mg^{2+} (Fig. 7 B). The kinetics of this component were voltage dependent and Mg^{2+} sensitive. Q_{OFF} reached its maximum value more quickly in the absence than in the presence of Mg^{2+} at all test potentials (Fig. 7 B). These results reveal that Mg^{2+} slows the kinetics of ON gating currents in eag, but the effect is much smaller than on ionic current kinetics (Fig. 2 C).

A quantitative discrepancy between the effect of Mg^{2+} on ionic and gating current kinetics was also seen using the reactivation protocol. Although Mg^{2+} dramatically slowed the reactivation time course of ionic cur-

Figure 7. Slow component of ON gating charge movement is enhanced by Mg^{2+}. (A) From a holding potential of -90 mV, 70-ms test pulses from -30 to $+50$ mV were applied in 10-mV increments. Time constants, obtained from single exponential components of the decaying phase of ON gating currents recorded in the presence (●) or absence (○) of 2 mM Mg^{2+}, are plotted versus test potential. These time constants describe a fast component of charge movement that is not significantly changed by Mg^{2+}. Data are shown as mean $\pm$ SEM, $n = 4$. (B) From a holding potential of -90 mV, ON gating currents were evoked by test pulses of various durations between 2 and 100 ms to $+20$, 0, or -20 mV. After each pulse, OFF gating currents were evoked by a return to -90 mV. OFF gating currents, obtained in the presence (●) or absence (○) of 2 mM Mg^{2+}, were integrated to obtain Q_{OFF}, which was normalized to the maximal value obtained at the same test potential in the presence or absence of Mg^{2+} and plotted versus test pulse duration. A slowly developing component of charge movement is more prominent in the presence of Mg^{2+}, especially at smaller depolarizations. Data are shown as mean $\pm$ SEM, $n = 4$.
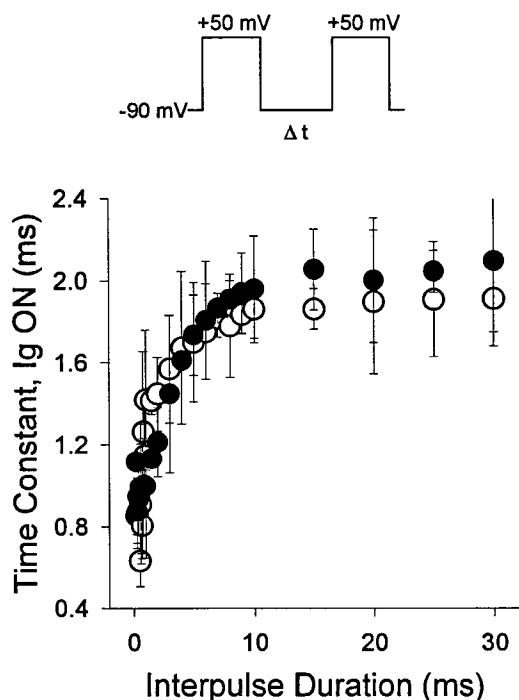
Figure 8. Mg^{2+} does not significantly modulate gating current reactivation time course. Gating currents were recorded using the reactivation protocol shown in Fig. 4. The decay phase of ON gating currents evoked by the second test pulse in the presence (●) or absence (○) of 2 mM Mg^{2+} were fitted with single exponential functions. Fitted time constants are plotted versus Δt. Data are shown as mean ± SEM, $n = 3$.

rents (Fig. 4), reactivation kinetics of ON gating currents were not sensitive to extracellular Mg^{2+} (Fig. 8).

The results described in this section suggest that Mg^{2+} modulates gating transitions that occur slowly and/or move relatively little charge. These are likely to include the rate-limiting transitions accessed by prepulse hyperpolarization.

Role of the S3–S4 Loop in Mg^{2+} Modulation of eag Gating

In the bovine homolog of eag, alternatively spliced variants differing in the length of the S3–S4 loop are differentially sensitive to extracellular Mg^{2+} (Frings et al., 1998). In addition, mutations in the S3–S4 loop dramatically modify the gating properties of eag channels (Tang et al., 1996, 1998; Tang and Papazian, 1997; Schönherr et al., 1999). Therefore, we investigated whether loop mutations altered the Mg^{2+} sensitivity of activation gating in *Drosophila* eag.

When bound to proteins, Mg^{2+} is often chelated by carboxylate side chains (da Silva and Williams, 1991). Frings et al. (1998) have proposed that acidic residues in the S3–S4 loop of bovine eag might contribute to the Mg^{2+} binding site. In *Drosophila* eag, the S3–S4 loop contains a sequence of mostly negatively charged residues, DRDED, corresponding to residues 333–337

(Warmke et al., 1991). We therefore investigated whether eag remains Mg^{2+} sensitive upon deletion of residues 333–337 (Δ333–337) (Tang and Papazian, 1997). This deletion shifts activation in the depolarized direction, consistent with a small surface charge effect on the voltage sensor (Tang and Papazian, 1997). In addition, Δ333–337 slows the activation kinetics of eag (Fig. 9 A). In contrast to their effect on wild-type eag, hyperpolarizing prepulses increased the delay but did not affect the time course of Δ333–337 ionic currents elicited by a subsequent depolarization (Fig. 9 B). Activation time constants, estimated by fitting a single exponential function to the late phase of ionic current records, did not differ significantly as a function of prepulse potential (Fig. 9 B). The increase in the delay was reflected by an increase in the time to half maximal current amplitude after more negative prepulses (Fig. 9 B). These results suggest that the transitions between closed states populated at hyperpolarized potentials are no longer rate limiting for activation in Δ333–337 channels. However, activation kinetics were still modulated by extracellular Mg^{2+} in Δ333–337 channels (Fig. 9 C). Thus, the DRDED sequence does not contribute significantly to the Mg^{2+} binding site in eag channels. Measurement of gating currents from the Δ333–337 mutant was not feasible because of the slow activation kinetics and low expression of this construct.

Consistent with these results, we note that Mg^{2+} does not significantly modulate the gating of *Shaker* or other voltage-dependent K$^+$ channels that are not members of the eag subfamily. It is worth noting that negatively charged sequences are also found in the analogous location in other voltage-dependent K$^+$ channels, including *Shaker* (Tempel et al., 1987). Therefore, sensitivity to Mg^{2+} does not correlate with the presence of negatively charged amino acids after segment S3.

In contrast to the Δ333–337 deletion, another mutation in the S3–S4 loop, L342H, eliminated the modulation of eag activation gating by prepulse hyperpolarization and extracellular Mg^{2+}. As previously described, the steady state and kinetic properties of activation in L342H, measured from ionic current recordings, are similar to those of wild-type eag (Tang et al., 1996, 1998; Tang and Papazian, 1997). However, hyperpolarizing prepulses from −90 to −200 mV altered neither the delay nor the time course of ionic currents evoked by a subsequent depolarization (Fig. 10 A). Furthermore, activation kinetics were not modulated by 2 mM extracellular Mg^{2+}, either in the presence or absence of hyperpolarizing prepulses (Fig. 10, A and B). Mg^{2+} concentrations up to 10 mM were tested and found to have no effect on activation kinetics in the L342H mutant (data not shown). One interpretation of these results is that the L342H mutation eliminates from the activation pathway transitions that are accessed at hyperpolarized
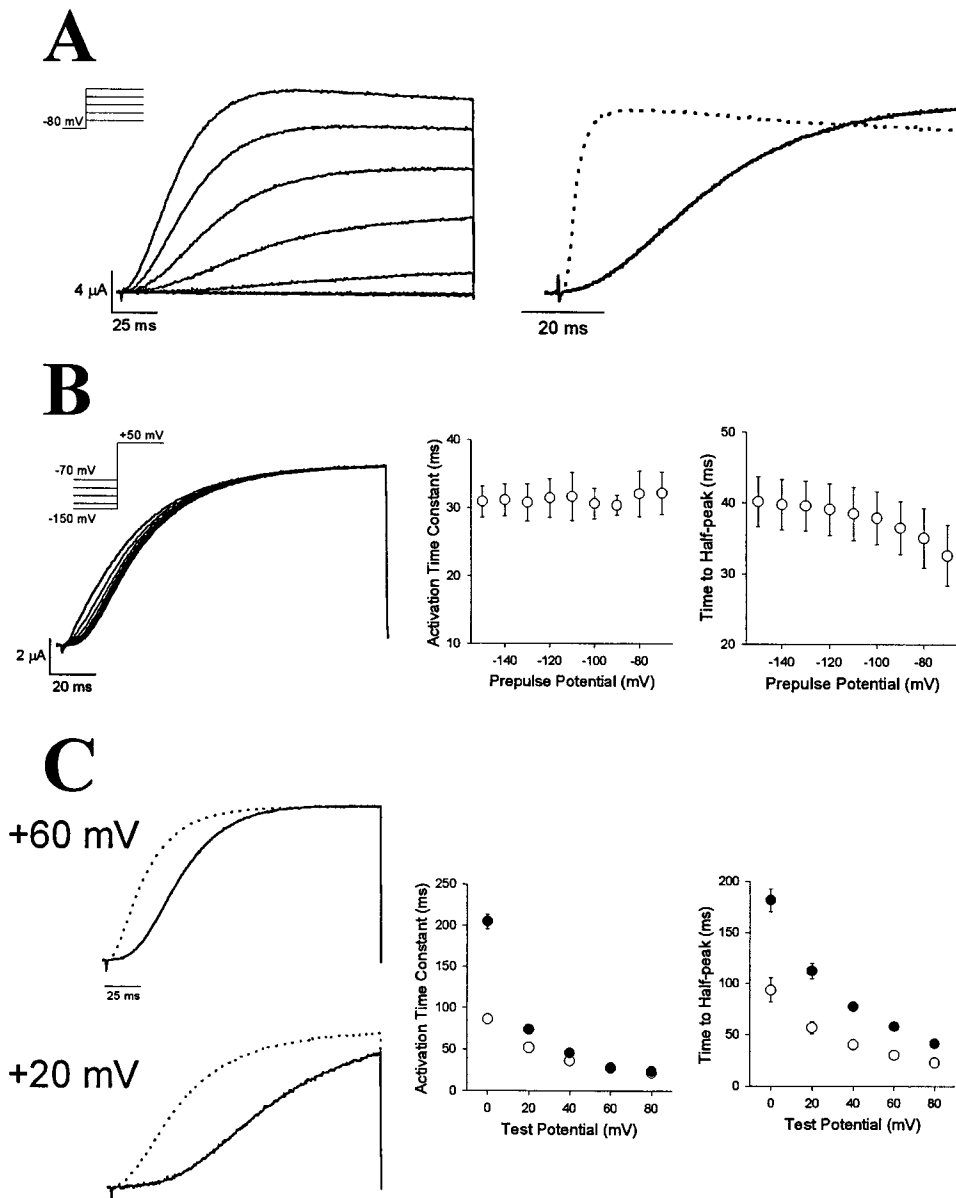
Figure 9. Δ333–337 activation kinetics are sensitive to Mg^{2+} but unaltered by prepulse hyperpolarization. (A, left) Ionic currents from the Δ333–337 mutant were evoked by pulsing from a holding potential of −80 mV to voltages from −60 to +80 mV in 20-mV increments. Representative traces, 150 ms in length, are shown. (Right) Currents evoked at +60 mV from Δ333–337 (solid trace) and wild-type eag (dashed trace) have been overlaid. (B) Prepulse hyperpolarization increases the delay but does not alter activation kinetics in Δ333–337 channels. (Left) From a holding potential of −80 mV, 150-ms hyperpolarizing prepulses ranging from −150 to −70 mV were applied in 10-mV increments, followed by a 120-ms test pulse to +50 mV. Representative currents evoked by the test pulses are shown. (Middle) Activation time constants at +50 mV, determined by fitting a single exponential function to the late rising phase, have been plotted as a function of prepulse potential. Data are shown as mean ± SEM, $n = 6$. (Right) To illustrate the effect of hyperpolarizing prepulses on the delay before current activation, the time to half maximal current amplitude at +50 mV has been plotted as a function of prepulse potential. Data are shown as mean ± SEM, $n = 6$. (C) Comparison of activation kinetics of Δ333–337 channels in the presence and absence of Mg^{2+}. (Left) Representative currents from Δ333–337 channels, evoked by pulses to +60 or +20 mV, as indicated, in the presence (solid traces) or absence (dashed traces) of 2 mM Mg^{2+}, have been overlaid. (Middle) Activation time constants at +50-mV pulse in the presence (●) or absence (○) of 2 mM Mg^{2+}, determined by fitting a single exponential function to the late rising phase, have been plotted as a function of test potential. Data are shown as mean ± SEM, $n = 8$. (Right) The time to half maximal current amplitude at +50 mV in the presence (●) or absence (○) of 2 mM Mg^{2+} has been plotted as a function of prepulse potential. Data are shown as mean ± SEM, $n = 8$.

potentials and modulated by Mg^{2+} in the wild-type channel. Interestingly, in a bovine homologue of eag, a mutation analogous to L342H also abolishes Mg^{2+} modulation of ionic current kinetics (Schönherr et al., 1999).

To determine whether the opening transition was still sensitive to Mg^{2+} in the L342H mutant, a reactivation experiment was performed. The kinetics of opening, estimated at very short interpulse intervals, were unaffected by Mg^{2+} in L342H channels (Fig. 10 C). Furthermore, activation kinetics during the second pulse returned to that seen in the first pulse at the same rate in the presence and absence of Mg^{2+} (Fig. 10 D). These results indicate that the L342H mutation abolishes the effect of Mg^{2+} on activation of the ionic currents in eag.

We also investigated whether the L342H mutation eliminates modulation of gating current kinetics by prepulse hyperpolarization and Mg^{2+} (Fig. 11). In the presence or absence of extracellular Mg^{2+}, hyperpolarizing prepulses did not significantly change the kinetics of ON gating currents (Fig. 11 A). The normalized decay kinetics of the ON gating currents in mutant and wild-type channels are compared as a function of prepulse potential in Fig. 11 B. Furthermore, Mg^{2+} did not modulate the development of a slow component of

A

0 mM Mg²⁺   2 mM Mg²⁺

$+50$ mV

-90 mV

-200 mV

2 μA

20 ms

B

0 mM Mg²⁺   2 mM Mg²⁺

-90 mV

0.2 μA

10 ms

C

Reactivation Time Constant (ms) vs Interpulse Interval (ms)

D

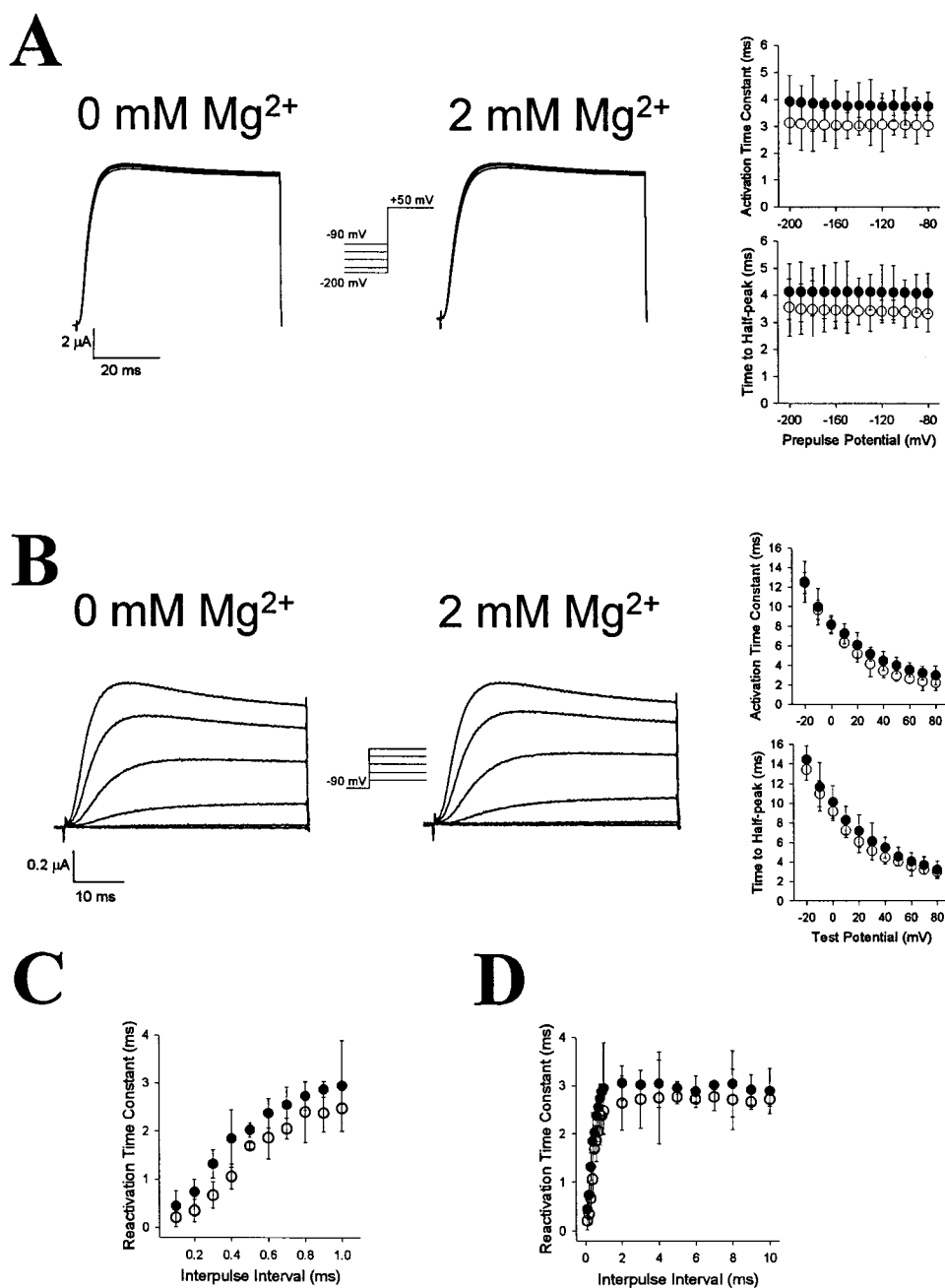Reactivation Time Constant (ms) vs Interpulse Interval (ms)

Figure 10. Ionic current activation kinetics in the L342H mutant are insensitive to both Mg²⁺ and prepulse hyperpolarization. (A, left and middle) Effect of hyperpolarizing prepulses on L342H currents. The voltage protocol was the same as in Fig. 1. Representative currents evoked by the test pulses in the presence or absence of 2 mM Mg²⁺, as indicated, are shown. (Right) Activation time constants (top) and time to half maximal current (bottom) in the presence (●) or absence (○) of Mg²⁺ have been plotted as a function of prepulse potential. Data are shown as mean ± SEM, $n = 6$. (B, left and middle) Currents were evoked in the presence or absence of 2 mM Mg²⁺, as indicated, by pulses from a holding potential of -90 mV. The voltage protocol was the same as in Fig. 2. (Right) Activation time constants (top) and time to half maximal current (bottom) in the presence (●) or absence (○) of 2 mM Mg²⁺ have been plotted as a function of test potential. Data are shown as mean ± SEM, $n = 6$. (C) L342H channels were subjected to the reactivation protocol shown in Fig. 4. Fitted time constants for the late rising phase of currents evoked by the second test pulse were determined for short interpulse intervals (between 0.1 and 1 ms) in the presence (●) and absence (○) of 2 mM Mg²⁺ and plotted versus Δt. Data are shown as mean ± SEM, $n = 5$. (D) Fitted time constants for the second test pulse were determined for interpulse intervals between 0.1 and 10 ms in the presence (●) and absence (○) of 2 mM Mg²⁺ and plotted versus Δt. Data are shown as mean ± SEM, $n = 5$.

Q_{OFF} after long depolarizations (Fig. 12). These results confirm that the L342H mutation greatly attenuates or eliminates the modulation of activation gating by Mg²⁺ and prepulse hyperpolarization.

DISCUSSION

Qualitative Model of Activation Gating in eag

Unlike other voltage-dependent K⁺ channels, activation gating in the *Drosophila* eag channel and its mammalian homologues is dramatically modulated by extracellular

Mg⁺² (Terlau et al., 1996; Frings et al., 1998; Meyer and Heinemann, 1998). In this study, we have characterized the effects of Mg²⁺ and prepulse hyperpolarization on the ionic and gating currents of eag. We find that Mg²⁺ regulates slow gating transitions that occur at hyperpolarized potentials. In addition, Mg²⁺ affects transitions involved in channel opening. Our most striking result is that, although the effects of Mg²⁺ and hyperpolarization on eag ionic and gating currents are qualitatively similar, the effects on gating currents are quantitatively much smaller than the effects on ionic currents.
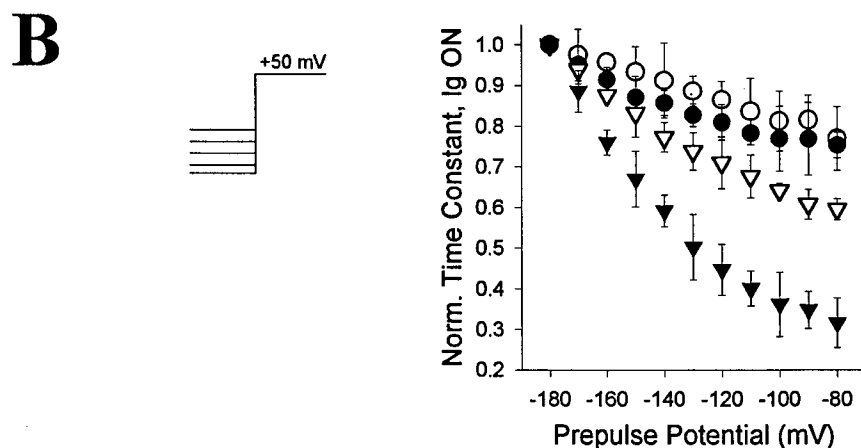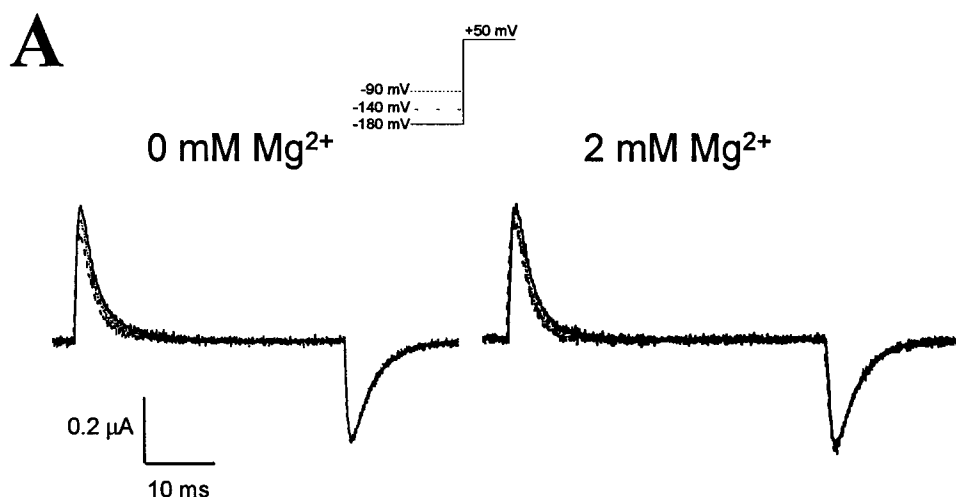
A

0 mM Mg^{2+} 2 mM Mg^{2+}

+50 mV

-90 mV
-140 mV
-180 mV

0.2 μA

10 ms

B

+50 mV

Norm. Time Constant, τg ON

Prepulse Potential (mV)

Figure 11. Gating currents recorded from L342H channels are insensitive to Mg^{2+} and prepulse hyperpolarization. (A) L342H gating currents were evoked by test pulses to +50 ms after prepulses to hyperpolarized potentials between −180 and −90 mV in the presence or absence of Mg^{2+}, as indicated. The voltage protocol was the same as in Fig. 6. (B) The decay phase of ON gating currents evoked at +50 mV was fitted with a single exponential function to derive a time constant, which was normalized to the value obtained after a prepulse to −180 mV, and plotted versus prepulse potential. wild-type eag (▽, ▼) and L342H (○, ●) in the absence (○, ▽) or presence (●, ▼) of 2 mM Mg^{2+}. Data are shown as mean ± SEM, $n = 3$.

Models for the gating of voltage-dependent K$^+$ channels generally postulate sequential, charge-moving transitions between closed states. These steps prime the channel for opening (Bezanilla et al., 1994; Zagotta et al., 1994b; Schoppa and Sigworth, 1998). A less voltage-dependent, cooperative transition is then required to enter the conducting state (Smith-Maxwell et al., 1998; Ledwell and Aldrich, 1999). An important question is whether a sequential model can account for the properties of eag ionic and gating currents in the presence and absence of Mg^{2+}. In particular, can the differential effects of hyperpolarization and Mg^{2+} on eag ionic and gating currents be qualitatively simulated using a sequential model for activation?

To address this question, we adapted a qualitative model for eag gating from the class D model previously proposed by Zagotta et al. (1994b) for *Shaker* channels. The model is presented in a condensed format that highlights conformational transitions that occur within each subunit of the channel (Fig. 13). For simplicity, the model assumes that the activation pathway consists of two independent and sequential gating transitions that occur identically in each subunit ($C_0 \leftrightarrow C_1$ and $C_1 \leftrightarrow C_2$ in the condensed model). Once all four subunits are in the C_2 state, the channel is in a conformation permissive for opening, designated C_2^*. A final, concerted conformational change opens the channel ($C_2^* \leftrightarrow O$).

In the model, the C_0 conformation is populated at hyperpolarized potentials. The first gating transition, $C_0 \leftrightarrow C_1$, is the rate-limiting step in the pathway, in accordance with the effects of hyperpolarizing prepulses on activation kinetics. This transition moves less gating charge than the second transition, $C_1 \leftrightarrow C_2$, which is responsible for the bulk of the detectable gating charge movement in eag. Opening of the pore, $C_2^* \rightarrow O$, is the fastest transition in the pathway, consistent with the results of reactivation experiments, which demonstrate that opening is not rate limiting in eag channels. We have assumed that pore opening occurs much faster than the reverse transition, $O \rightarrow C_2^*$.

The idea that the opening transition is much faster than the reverse reaction has previously been incorpo-
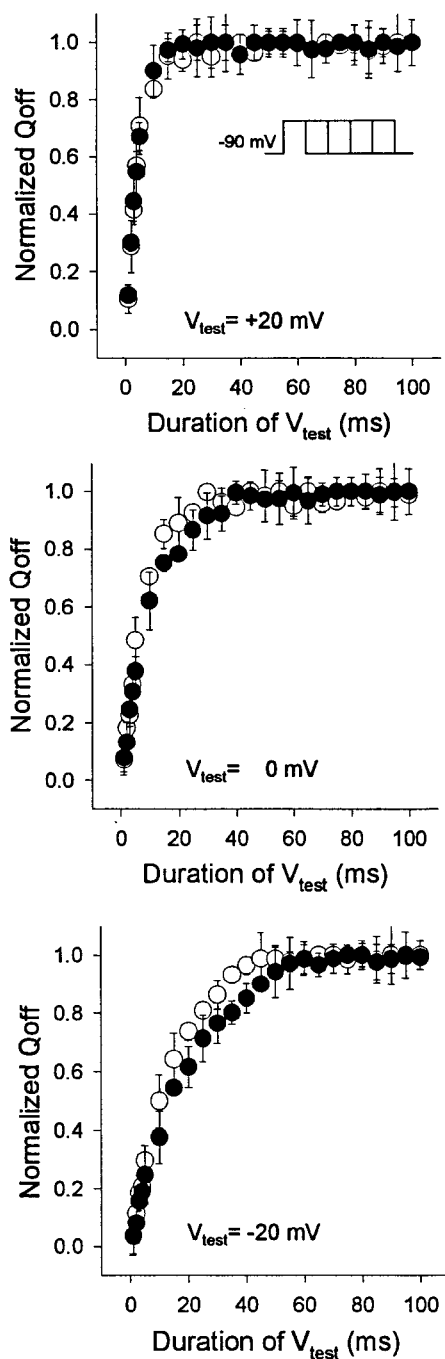
Figure 12. In L342H, the slow component of ON gating charge movement is not significantly modulated by Mg^{2+}. The voltage protocol was the same as in Fig. 7 B. OFF gating currents, recorded in the presence (●) or absence (○) of 2 mM Mg^{2+} at the indicated test potentials, were integrated to obtain Q_{OFF}, which was normalized to the maximal value obtained at the same test potential in the presence or absence of Mg^{2+} and plotted versus test-pulse duration. Data are shown as mean ± SEM, $n = 3$.
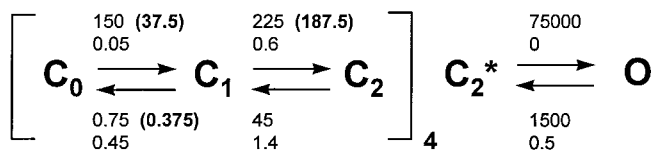

Figure 13. A qualitative, sequential model for activation gating in eag channels. The model is modified from the class D model proposed by Zagotta et al. (1994b) for the *Shaker* K^+ channel. Values for rate constants (s^{-1}; top number) and valences (bottom number) used in the simulation in the absence of Mg^{2+} are shown above the arrow for forward transitions and below the arrow for reverse transitions. Values for those parameters changed in the presence of 2 mM Mg^{2+} are shown in bold type in the brackets. The simulation employed a total gating charge of 10.5 e_0 per channel, a reasonable value compared to the charge per channel ($\sim$12 e_0) estimated experimentally for *Shaker* K^+ channels and skeletal muscle Na^+ channels (Schoppa et al., 1992; Hirschberg et al., 1995).

rated into models describing the gating of *Shaker* channels (Bezanilla et al., 1994; Zagotta et al., 1994b; Schoppa and Sigworth, 1998). In both *Shaker* and eag channels, ionic current deactivation and OFF gating currents have the same time course (Fig. 5 E; Bezanilla et al., 1991). This suggests that effective closing of the channel requires the return of much of the detectable gating charge to its resting conformation. In the model, this would correspond to transitions from O through C_2 to the C_1 state.

Our data suggest that Mg^{2+} slows at least two steps in the activation pathway, including rate-limiting transitions between closed states populated at hyperpolarized potentials and the transition from a nearby closed state(s) to the open state. Although the kinetics of ionic tail currents were unaffected by Mg^{2+}, the reactivation experiment demonstrated that Mg^{2+} decelerates one or more back transitions between closed states. Mg^{2+} modulation of activation kinetics was simulated by reducing the rates of the forward and backward transitions between C_0 and C_1, and to a lesser extent the forward transition from C_1 to C_2. According to the model, once the channel reaches the C_2* state, the pore opens rapidly. Therefore, slowing the $C_1 \rightarrow C_2$ transition can account for the effect of Mg^{2+} on pore opening. In the simulation, the fast kinetics of the C_2* to O transition were unchanged by Mg^{2+}.

This model is not intended to provide a quantitative or complete description of eag gating. In particular, it does not reproduce the complicated, sigmoid kinetics of the initial phase of activation of eag ionic currents, which would require additional transitions. Importantly, however, simulations using this model can reproduce the quantitatively larger effects of Mg^{2+} and hyperpolarizing prepulses on ionic than on gating currents and key features of eag ionic and gating currents, including the deceleration of activation kinetics after hyperpolarizing prepulses and the effect of Mg^{2+} on activation and reactivation kinetics (Fig. 14).
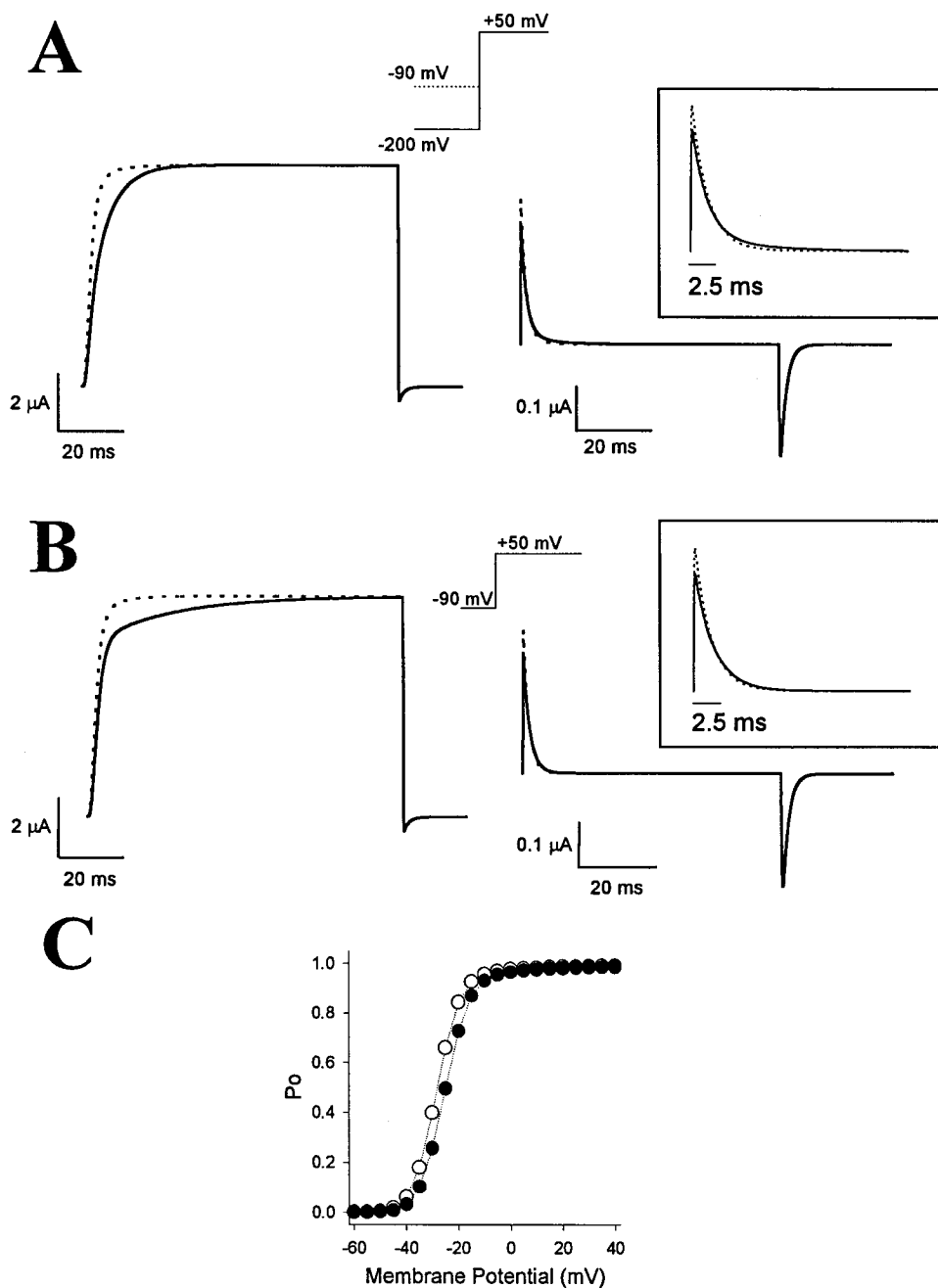
Figure 14. Computer simulation of the modulation of eag ionic and gating currents by prepulse hyperpolarization and extracellular Mg^{2+}. (A) Simulated effect of prepulse hyperpolarization on ionic (left) and gating (right) currents. A prepulse of -90 mV (dashed line) or -200 mV (solid line) is applied before a test pulse to $+50$ mV. At the end of the test pulse, the membrane is repolarized to -90 mV. The reversal potential is set at -80 mV. An enlarged view of ON gating currents is provided (right inset) to show the effect of the prepulse on the decay kinetics. (B) Simulated ionic (left) and gating (right) currents in the presence (solid line) and absence (dashed line) of 2 mM Mg^{2+}. From a holding potential of -90 mV, a test to pulse to $+50$ mV is applied, followed by repolarization to -90 mV. The reversal potential is set at -80 mV. An enlarged view of ON gating currents is provided (right inset) to show the effect of Mg^{2+} on the decay kinetics. (C) The predicted steady state P_o-V curve in the presence (●) or absence (○) of 2 mM Mg^{2+} is shown.

Shown in Fig. 14 A is the simulated effect of a prepulse to -200 mV before a test pulse to $+50$ mV. The time courses of ionic currents evoked with and without the prepulse cannot be superimposed by sliding the traces along the time axis (Fig. 14 A, left). Thus, the model confirms that this feature can result from rate-limiting transitions between closed states populated at hyperpolarized potentials. Importantly, the model predicts that the same prepulse protocol results in a much smaller effect on the kinetics of ON gating currents (Fig. 14 A, right).

The simulated effect of Mg^{2+} on activation kinetics is shown in Fig. 14 B. In accord with our experimental re-

sults, the model predicts that Mg^{2+} slows activation kinetics of ionic currents without changing tail current kinetics (Fig. 14 B, left). Significantly, Mg^{2+} has a minimal effect on gating current kinetics in the simulation (Fig. 14 B, right). Also in agreement with the data, Mg^{2+} has little effect on the steady state voltage dependence of the channel (Fig. 14 C).

The model predicts that the effect of Mg^{2+} on ionic and gating currents is less prominent at more positive test potentials and that Mg^{2+} enhances the effects of prepulse hyperpolarization (not shown). These features are consistent with our experimental findings (Figs. 2, 3, 6, and 7).

The model also predicts the effect of Mg^{2+} on the reactivation kinetics of eag ionic currents (not shown). In particular, slowing the back transition from C_1 to C_0 can account for our observation that a longer interpulse interval is required for activation kinetics to return to their original rate in the presence of Mg^{2+}. Furthermore, decelerating the $C_1 \to C_2$ transition in the presence of Mg^{2+} results in slower reactivation kinetics even at very short interpulse intervals, accounting for the apparent effect of Mg^{2+} on pore opening.

The simulation results indicate that a sequential activation model can account for the differential effects of hyperpolarization and Mg^{2+} on eag ionic and gating currents.

It is worth noting that our data do not rule out the possibility that the quantitatively larger effect of Mg^{2+} on ionic than gating currents is due to some kind of antagonistic interaction between Mg^{2+} and TEA. Such an interaction would affect gating current but not ionic current measurements. To address this possibility, we attempted to record gating currents after complete replacement of internal and external K^+ by NMG. Such attempts were unsuccessful. Using the cut-open oocyte approach, eag ran down before K^+ was thoroughly replaced, making it infeasible to measure gating currents uncontaminated by ionic currents. Run down of eag in excised patches has been previously reported (Robertson et al., 1996). In ionic current experiments, we found that a submaximal dose of TEA did not alter modulation of activation kinetics by extracellular Mg^{2+} (data not shown).

Terlau et al. (1996) previously proposed a gating model for the rat homolog of eag, based on measurements of ionic currents. They postulated that Mg^{2+} regulates a voltage-dependent transition between slow and fast gating modes, slowing the forward transition and speeding the back transition. These kinetic changes would be expected to alter the equilibrium between closed and open states, shifting the voltage dependence of the channel in the depolarized direction. In contrast, our model predicts little shift in the P_o-V curve in the presence of Mg^{2+} (Fig. 14 C), in accordance with our data (Fig. 5 D).

Role of the S3–S4 Loop in the Voltage-dependent Gating of eag

Mutations in the S3–S4 loop strongly influence the steady state voltage dependence of eag (Tang and Papazian, 1997). The present results indicate that mutations in the region also significantly alter the activation rate and its regulation by Mg^{2+}. It is worth noting that the S3–S4 loop also plays a role in the activation of other K^+ channels. The steady state voltage dependence of Kv2.1 is modified by a toxin that binds to this region (Swartz and MacKinnon, 1997a,b), and mutations in

the *Shaker* S3–S4 loop alter activation kinetics (Mathur et al., 1997; Gonzalez et al., 1999).

The L342H mutation virtually eliminates the modulation of eag ionic and gating currents by Mg^{2+}. It is unlikely that the original leucine side chain is directly involved in coordination of the Mg^{2+} ion, although mutating the residue may indirectly alter the architecture of the binding site. Alternatively, the mutation may block access to the site or dramatically reduce the kinetic prominence of the Mg^{2+}-sensitive steps in the gating mechanism. At present, we cannot distinguish between these possibilities.

Comparison of Activation Gating in eag and Other Voltage-dependent K^+ Channels

The properties of gating currents in eag channels resemble those previously described in other voltage-dependent K^+ channels such as *Shaker*. Gating currents recorded from *Shaker* and eag channels are characterized by a rising phase, indicating that early steps in the activation pathway move less charge than later transitions (Bezanilla et al., 1991; Zagotta et al., 1994a; Schoppa and Sigworth, 1998). In *Shaker* channels, the gating charge moves in at least two interdependent phases differing in their steady state and kinetic properties (Bezanilla et al., 1994). The early phase of gating, associated with movement of the q_1 component of gating charge, occurs at hyperpolarized potentials, moves approximately one third of the gating charge, and is the faster of the two resolved kinetic components of charge movement. This phase is responsible for the delay in activation after hyperpolarizing prepulses. In contrast, the q_2 phase of gating has a voltage dependence similar to activation of the ionic conductance, moves approximately two thirds of the gating charge, and is the slower of the two resolved kinetic components. The rising phase in eag gating currents suggests that the charge movement detected in eag also consists of at least two phases, although additional experiments will be required to determine whether components analogous to q_1 and q_2 can be detected in eag channels. If so, one important difference between gating in *Shaker* and eag channels is that transitions occurring at more hyperpolarized potentials are rate limiting for eag activation, which is not the case in *Shaker* channels.

REFERENCES

Aggarwal, S.K., and R. MacKinnon. 1996. Contribution of the S4 segment to the gating charge in the *Shaker* K$^+$ channel. *Neuron* 16:1169–1177.

Armstrong, C.M., and F. Bezanilla. 1973. Currents related to movement of the gating particles of sodium channels. *Nature.* 242: 459–461.

Armstrong, C.M., and F. Bezanilla. 1977. Inactivation of the sodium channel: II. Gating current experiments. *J. Gen. Physiol.* 70:567–590.

Bezanilla, F., and C.M. Armstrong. 1977. Inactivation of the sodium channel: I. Sodium current experiments. *J. Gen. Physiol.* 70:549–566.

Bezanilla, F., E. Perozo, D.M. Papazian, and E. Stefani. 1991. Molecular basis of gating charge immobilization in *Shaker* potassium channels. *Science.* 254:679–683.

Bezanilla, F., E. Perozo, and E. Stefani. 1994. Gating of *Shaker* K$^+$ channels. II. The components of gating currents and a model of channel activation. *Biophys. J.* 66:1011–1021.

Brüggemann, A., L.A. Pardo, W. Stühmer, and O. Pongs. 1993. Ether-à-go-go encodes a voltage-gated channel permeable to K$^+$ and Ca^{2+} and modulated by cAMP. *Nature.* 365:445–448.

Cha, A., and F. Bezanilla. 1997. Characterizing voltage-dependent conformational changes in the *Shaker* K$^+$ channel with fluorescence. *Neuron.* 19:1127–1140.

Chen, F.S.P., D. Steele, and D. Fedida. 1997. Allosteric effects of permeating cations on gating currents during K$^+$ channel deactivation. *J. Gen. Physiol.* 110:87–100.

Cole, K.S., and J.W. Moore. 1960. Potassium ion current in the squid giant axon: dynamic characteristic. *Biophys. J.* 1:1–14.

da Silva, J.J.R.F., and R.J.P. Williams. 1991. The biological chemistry of magnesium: phosphate metabolism. *In* The Biological Chemistry of the Elements: the Inorganic Chemistry of Life. Oxford University Press, New York, New York. 166–267.

Frings, S., N. Brüll, C. Dzeja, A. Angele, V. Hagen, U.B. Kaupp, and A. Baumann. 1998. Characterization of ether-à-go-go channels present in photoreceptors reveal similarity to I$_{Kx}$, a K$^+$ current in rod inner segments. *J. Gen. Physiol.* 111:583–599.

Gonzalez, C., J. Amigo, E. Rosenmann, F. Bezanilla, O. Alvarez, and R. Latorre. 1999. Role of the S3–S4 linker in the activation of *Shaker* K$^+$ channels. *Biophys. J.* 76:A78. (Abstr.)

Hirschberg, B., A. Rovner, M. Lieberman, and J. Patlak. 1995. Transfer of twelve charges is needed to open skeletal muscle Na$^+$ channels. *J. Gen. Physiol.* 106:1053–1068.

Hodgkin, A.L., and A.F. Huxley. 1952. A quantitative description of membrane current and its application to conduction and excitation in nerve. *J. Physiol.* 117:500–544.

Larsson, H.P., O.S. Baker, D.S. Dhillon, and E.Y. Isacoff. 1996. Transmembrane movement of the *Shaker* K$^+$ channel S4. *Neuron.* 16:387–397.

Ledwell, J.L., and R.W. Aldrich. 1999. Mutations in the S4 region isolate the final voltage-dependent cooperative step in potassium channel activation. *J. Gen. Physiol.* 113:389–414.

Liman, E.R., P. Hess, F. Weaver, and G. Koren. 1991. Voltage-sensing residues in the S4 region of a mammalian K$^+$ channel. *Nature.* 353:752–756.

Ludwig, J., H. Terlau, F. Wunder, A. Brügemann, L.A. Pardo, A. Marquardt, W. Stühmer, and O. Pongs. 1994. Functional expression of a rat homologue of the voltage gated ether-à-go-go potassium channel reveals differences in selectivity and activation kinetics between the *Drosophila* channel and its mammalian counterpart. *EMBO (Eur. Mol. Biol. Organ.) J.* 13:4451–4458.

MacKinnon, R. 1991. Determination of the subunit stoichiometry of a voltage-activated potassium channel. *Nature.* 350:232–235.

Mannuzzu, L.M., M.M. Moronne, and E.Y. Isacoff. 1996. Direct physical measure of conformational rearrangement underlying potassium channel gating. *Science.* 271:213–216.

Mathur, R., J. Zheng, Y. Yan, and F.J. Sigworth. 1997. Role of the S3–S4 linker in *Shaker* potassium channel activation. *J. Gen. Physiol.* 109:191–199.

Meyer, R., and S.H. Heinemann. 1998. Characterization of an eag-like potassium channel in human neuroblastoma cells. *J. Physiol.* 508:49–56.

Olcese, R., R. Latorre, L. Toro, F. Bezanilla, and E. Stefani. 1997. Correlation between charge movement and ionic current during slow inactivation in *Shaker* K$^+$ channels. *J. Gen. Physiol.* 110:579–589.

Oxford, G.S. 1981. Some kinetic and steady state properties of sodium channels after removal of inactivation. *J. Gen. Physiol.* 77: 1–22.

Papazian, D.M., and F. Bezanilla. 1997. How does an ion channel sense voltage? *News Physiol. Sci.* 12:203–210.

Papazian, D.M., L.C. Timpe, Y.N. Jan, and L.Y. Jan. 1991. Alteration of voltage-dependence of *Shaker* potassium channel by mutations in the S4 sequence. *Nature.* 349:305–310.

Robertson, G.A., J.W. Warmke, and B. Ganetzky. 1996. Potassium currents expressed from *Drosophila* and mouse eag cDNAs in *Xenopus* oocytes. *Neuropharmacology.* 35:841–850.

Schneider, M.F., and W.K. Chandler. 1973. Voltage-dependent charge movement of skeletal muscle, a possible step in excitation–contraction coupling. *Nature.* 242:244–246.

Schönherr, R., S. Hehl, H. Terlau, A. Baumann, and S.H. Heinemann. 1999. Individual subunits contribute independently to slow gating of bovine eag potassium channels. *J. Biol. Chem.* 274: 5362–5369.

Schoppa, N.E., and F.J. Sigworth. 1998. Activation of *Shaker* potassium channels. III. An activation gating model for wild-type and V2 mutant channels. *J. Gen. Physiol.* 111:313–342.

Schoppa, N.E., K. McCormack, M.A. Tanouye, and F.J. Sigworth. 1992. The size of gating charge in wild-type and mutant *Shaker* potassium channels. *Science.* 255:1712–1715.

Seoh, S.-A., D. Sigg, D.M. Papazian, and F. Bezanilla. 1996. Voltage-sensing residues in the S2 and S4 segments of the *Shaker* K$^+$ channel. *Neuron.* 16:1159–1167.

Smith-Maxwell, C.J., J.L. Ledwell, and R.W. Aldrich. 1998. Uncharged S4 residues and cooperativity in voltage-dependent potassium channel activation. *J. Gen. Physiol.* 111:421–439.

Starace, D., and F. Bezanilla. 1998. Accessibility studies of *Shaker* K channel S4 residues by histidine scanning mutagenesis. *Biophys. J.* 74:A254. (Abstr.)

Starace, D., E. Stefani, and F. Bezanilla. 1998. Histidine scanning mutagenesis indicates full translocation of two charges of the *Shaker* K channel voltage sensor. *Biophys. J.* 74:A215. (Abstr.)

Starace, D.M., E. Stefani, and F. Bezanilla. 1997. Voltage-dependent proton transport by the voltage sensor of the *Shaker* K$^+$ channel. *Neuron.* 19:1319–1327.

Stefani, E., L. Toro, E. Perozo, and F. Bezanilla. 1994. Gating of *Shaker* K$^+$ channels: I. Ionic and gating currents. *Biophys. J.* 66: 996–1010.

Stühmer, W., F. Conti, H. Suzuki, X. Wang, M. Noda, N. Yahagi, H. Kubo, and S. Numa. 1989. Structural parts involved in activation and inactivation of the sodium channel. *Nature.* 339:597–603.

Swartz, K.J., and R. MacKinnon. 1997a. Hanatoxin modifies the gating of a voltage-dependent K$^+$ channel through multiple binding sites. *Neuron.* 18:665–673.

Swartz, K.J., and R. MacKinnon. 1997b. Mapping the receptor site for hanatoxin, a gating modifier of voltage-dependent K$^+$ chan-

nels. *Neuron.* 18:675–682.

Taglialatela, M., and E. Stefani. 1993. Gating currents of the cloned delayed rectifier K$^+$ channel Drk1. *Proc. Natl. Acad. Sci. USA.* 90: 4758–4762.

Tang, C.-Y., F. Bezanilla, and D.M. Papazian. 1998. Gating currents in *Drosophila* eag K$^+$ channels: modulation by prepulse hyperpolarization and external Mg^{2+}. *Biophys. J.* 74:A240. (Abstr.)

Tang, C.-Y., and D.M. Papazian. 1997. Transfer of voltage independence from a rat olfactory channel to the *Drosophila* ether-à-go-go K$^+$ channel. *J. Gen. Physiol.* 109:301–311.

Tang, C.-Y., D. Sigg, F. Bezanilla, and D.M. Papazian. 1996. Gating currents in eag K$^+$ channels. *Biophys. J.* 70:A406. (Abstr.)

Tempel, B.L., D.M. Papazian, T.L. Schwarz, Y.N. Jan, and L.Y. Jan. 1987. Sequence of a probable potassium channel component encoded at *Shaker* locus of *Drosophila*. *Science.* 237:770–775.

Terlau, H., J. Ludwig, R. Steffan, O. Pongs, W. Stühmer, and S.H. Heinemann. 1996. Extracellular Mg^{2+} regulates activation of rat eag potassium channel. *Pflügers Arch.* 432:301–312.

Timpe, L.C., T.L. Schwarz, B.L. Tempel, D.M. Papazian, Y.N. Jan, and L.Y. Jan. 1988. Expression of functional potassium channels from *Shaker* cDNA in *Xenopus* oocytes. *Nature.* 331:143–145.

Warmke, J.W., and B. Ganetzky. 1994. A family of potassium channel genes related to eag in *Drosophila* and mammals. *Proc. Natl. Acad. Sci. USA.* 91:3438–3442.

Warmke, J., R. Drysdale, and B. Ganetzky. 1991. A distinct potassium channel polypeptide encoded by the *Drosophila* eag locus. *Science.* 252:1560–1562.

Yang, N., A.L. George, and R. Horn. 1996. Molecular basis of charge movement in voltage-gated sodium channels. *Neuron.* 16: 113–122.

Yang, N., and R. Horn. 1995. Evidence for voltage-dependent S4 movement in sodium channels. *Neuron.* 15:213–218.

Young, S.H., and J.W. Moore. 1981. Potassium ion currents in the crayfish giant axon: dynamic characteristics. *Biophys. J.* 36:723–733.

Zagotta, W.N., T. Hoshi, J. Dittman, and R.W. Aldrich. 1994a. *Shaker* potassium channel gating. II: Transitions in the activation pathway. *J. Gen. Physiol.* 103:279–319.

Zagotta, W.N., T. Hoshi, and R.W. Aldrich. 1994b. *Shaker* potassium channel gating. III: Evaluation of kinetic models for activation. *J. Gen. Physiol.* 103:321–362.